3
4
1

#2

UNITED STATES EXPERIMENTAL MODEL BASIN

NAVY YARD, WASHINGTON, D.C.

HYDRODYNAMIC CHARACTERISTICS OF TWELVE SYMMETRICAL HYDROFOILS (Rudders)

BY R. C. DARNELL

~~RESTRICTED~~

CONTENTS OF THIS REPORT NOT TO BE DIVULGED OR REFERRED TO IN ANY PUBLICATION. IN THE EVENT INFORMATION DERIVED FROM THIS REPORT IS PASSED ON TO OFFICER OR CIVILIAN PERSONNEL, THE SOURCE SHOULD NOT BE REVEALED.

NOVEMBER 1932 REPORT NO. 341

HYDRODYNAMIC CHARACTERISTICS of TWELVE SYMMETRICAL HYDROFOILS

- By R. C. Darnell -

U. S. Experimental Model Basin
Navy Yard, Washington, D. C.

November, 1932 Report No. 341.

INDEX

FIGURES AND TABLES

TABLE of SYMBOLS USED

A	area of hydrofoil
c	chord of hydrofoil or rudder width
b	span of hydrofoil or rudder depth
R	aspect ratio b^2/A
R_e	effective aspect ratio
v	velocity of hydrofoil through the water, ft. per sec. or knots
v_c	carriage speed for a particular run, ft. per sec or knots
α	angle of attack
R.N.	Reynolds' number = $\frac{cv}{\nu}$
ν	kinematic viscosity
D	measured drag in pounds
L	measured lift in pounds
Qm	measured torque in lb.in. (about rudder stock)
Q	torque about quarter-chord point in lb. in.
C_L	absolute coefficient of lift
C_D	absolute coefficient of drag
C_{M_o}	absolute coefficient of moment (about quarter-chord point)
C_{D_i}	coefficient of induced drag (absolute)
C_{Do}	coefficient of profile drag (absolute)
C.P.	center of pressure in per cent of chord from leading edge
F	dynamometer calibration constant for lift and drag
F_Q	dynamometer calibration constant for torque
K	factor correcting for wake
a	slope of C_L-curve per degree
a_o	slope of C_L-curve per degree for infinite aspect ratio
τ	factor correcting the induced angle of attack to allow for the departure from elliptical span loading resulting from the use of a rectangular span form.
ψ	angle of the resultant force acting on the hydrofoil with the normal to the plane of symmetry of the hydrofoil.
ρ	density of water – poundals per cu. ft.

HYDRODYNAMIC CHARACTERISTICS of TWELVE SYMMETRICAL HYDROFOILS

ABSTRACT

The center of pressure and absolute coefficients of lift, drag, and moment are given for twelve hydrofoils of symmetrical section and 0.25 sq. ft. area at a Reynolds' number of approximately 175,000. The hydrofoils were towed (leading edge vertical) in the tank of the Model Basin beneath a special flat-bottomed float that carried the dynamometer by which the lift, drag, and torque were measured. The angle of attack was varied from 0° to 45° and the gap between the top of the hydrofoil and the bottom of the float from 0 to 2 inches. The aspect ratios studied were 0.5, 1.0, 1.5, and 2.0. The effect of running the hydrofoils reversed was also studied.

In general the results show good agreement with data from wind tunnel tests.

I INTRODUCTION

The design of rudders and submarine diving planes has, in the past, been based almost entirely on the conventional flat plate formulas, either that of Joessel or a modification. Experience has shown that Joessel's does not accurately represent the true rudder forces, especially at large angles, and a correction is usually attempted by the introduction of a factor which varies from 0.45 to 0.75, depending upon the type, size, and speed of the ship, and which is based mainly upon designs of rudders and diving planes that have been found to be satisfactory.

Further, rudders of many modern ships and especially diving planes of modern submarines are of stream line form and considerable question has been raised as to the applicability of Joessel's formula which was formulated from measurements on flat plates. This question includes not only the forces on the rudders but also the position of the center of pressure which must be known in order to calculate the torque on the rudder stock and the stresses in the steering gear.

In view of these questions and a number of failures of rudders and diving planes, it became desirable to undertake an investigation of the subject. To this end the Experimental Model Basin has determined the lift, drag, and moment coefficients, as well as the center of pressure for twelve symmetrical stream line hydrofoils of varying aspect ratio, thickness ratio, and leading and trailing edge taper.

II APPARATUS and METHOD

General Outline of Method

The hydrofoils were towed (leading edge vertical) in the tank of the Model Basin beneath a specially constructed flat-bottomed float which carried the dynamometer by which the lift, drag, and torque were measured. The angle of attack was varied from 0° to 45° and the gap between the top of the hydrofoil and the bottom of the float from 0 to 2 in. In general, four sets of runs were made for each rudder, each covering the whole range of angle of attack, namely:

1. Rudder run forward – rudder clearance from hull 0 in.
2. " " reversed " " " " 0 "
3. " " forward " " " " 2 "
4. " " reversed " " " " 2 "

From the dynamometer readings of lift, drag, and torque, the absolute coefficients of lift, drag, and moment, were calculated as was also the L/D ratio and the position of the center of pressure.

Dynamometer Float

The lines of the rudder dynamometer float are shown in Fig. 1. The float is essentially a flat-bottomed boat with a square transom such that horizontal flow obtains at the stern in the region in which the hydrofoil is located. The float is 20 ft. long and has a beam of 31 in. Fig. 2 shows the stern of the float with the dynamometer and hydrofoil in position. For the tests the float was ballasted so as to give a draft at the transom of approximately two inches.

Dynamometer

The dynamometer, by which measurements of lift, drag, and torque were obtained, is shown in Figs. 3 and 4. It consists of a platform, to which the rudder stock bearing is secured, supported elastically above the base by means of two cylindrical springs and two pivot pins in such a manner that lateral and longitudinal translation as well as rotation about a vertical axis are possible. The magnitudes of these motions are a measure of the lift, drag, and torque respectively, and are determined by four dial gages mounted in pairs so as to measure the lateral and longitudinal flexure of each of the two springs. Calibration of the dynamometer by known forces is required before use; this is described in Appendix II.

The rudder stock is clamped to a sector of a worm and sector gear mounted on the movable platform and so arranged as to make possible the variation of the angle of attack from -5° to +45°. A moving scale attached to the sector gear indicates the angle of attack. Preliminary to placing the float in the water the scale was set at zero angle and the chord of the rudder lined up with the longi-

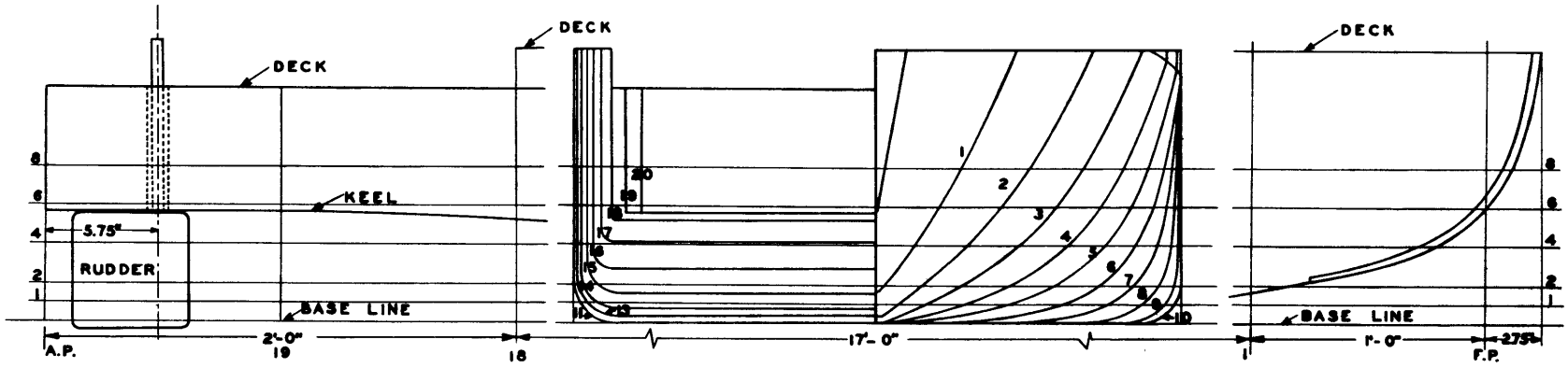

FIG. 1 RUDDER DYNAMOMETER FLOAT

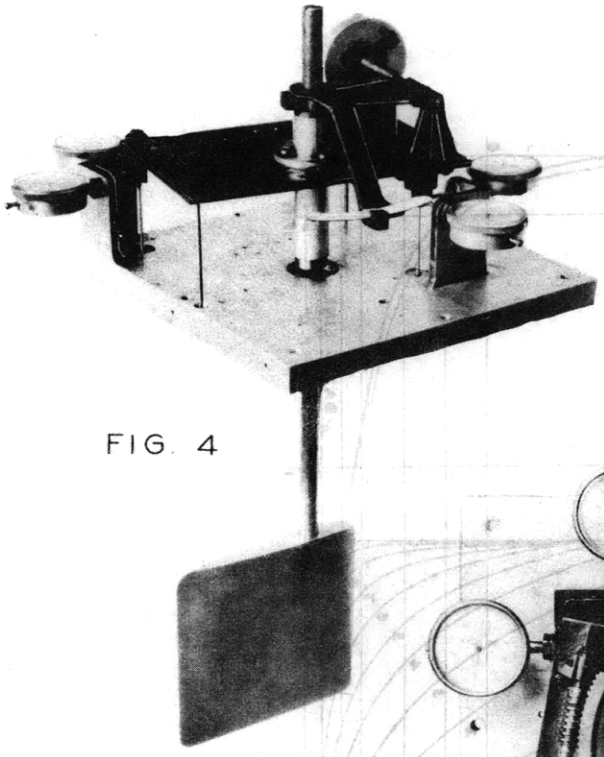

FIG. 4

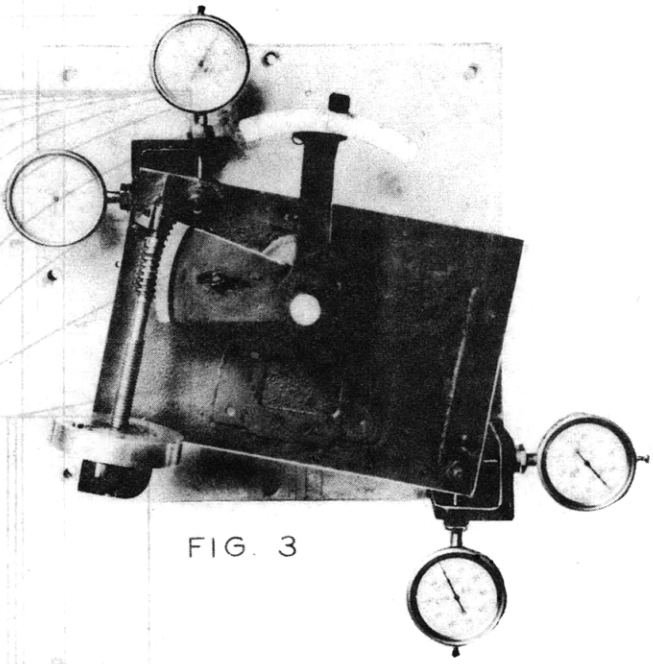

FIG. 3

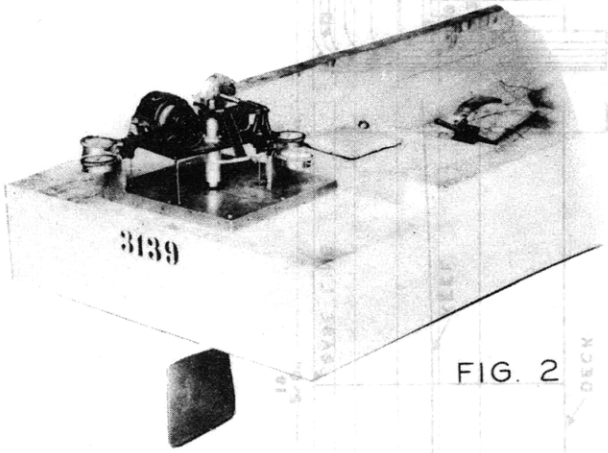

FIG. 2

tudinal center line of the float. The accuracy of the zero setting was probably within one degree and this error was corrected in the plotting of the data by shifting all curves by the amount necessary to make the curve of lift coefficient pass through the origin.

Description of Hydrofoils Tested

The plans of the twelve model rudders or hydrofoils that were tested were submitted by the Portsmouth Navy Yard and are shown in Figs. 5–8, inclusive. The rudders were so scaled that all have a projected area of very nearly 0.25 sq. ft. Rudders Nos. 8, 1, 10, and 9 represent aspect ratios of 0.5, 1.0, 1.5, and 2.0, respectively. Rudders Nos. 1, 2, and 3, all of aspect ratio 1.0, have thickness ratios of 0.10, 0.13, and 0.04, respectively; rudder No. 3 being, in effect, a flat plate with the leading edge rounded off and a slight thickening in the region of the quarter chord point to permit the attachment of the stock. Rudders Nos. 4, 5, 6, 7, 11, and 12 are tapered rudders, that is, the leading or trailing edge is tapered by 15° or 30° as the case may be.

The rudders were made of white metal cast about the stocks in accurately constructed wooden molds. No machining was necessary, all the finishing required being a slight smoothing of the surfaces with emery cloth.

III PROCEDURE of TEST

Preliminary Tests with Flat Plate

Rudder No. 3, which corresponds very closely to a flat plate, was first tested under a variety of conditions in order to determine the most favorable conditions for testing the series of rudders and to reveal any limitations of the apparatus or test method.

With the rudder mounted so that there was no clearance between the top of the rudder and the under-side of the hull, a run was made with the float so ballasted that the lower edge of the transom was just submerged in the water when at rest. As was anticipated, for angles of attack larger than 10°, the water failed to "close in" aft of the rudder. To prevent this the draft had to be increased to approximately 2 in. In the case of a few rudders at angles of attack of 35° or more, even this was not enough to prevent the formation of an air pocket (not to be confused with cavitation) caused by the failure of the water to close in. This resulted in an abrupt drop in the lift and drag curves at this point but, as tests had already been completed for most of the rudders, it was not desired to change the draft. Furthermore, the draft was as great as was conveniently possible; a further increase would have caused the float to ship water from the bow wave.

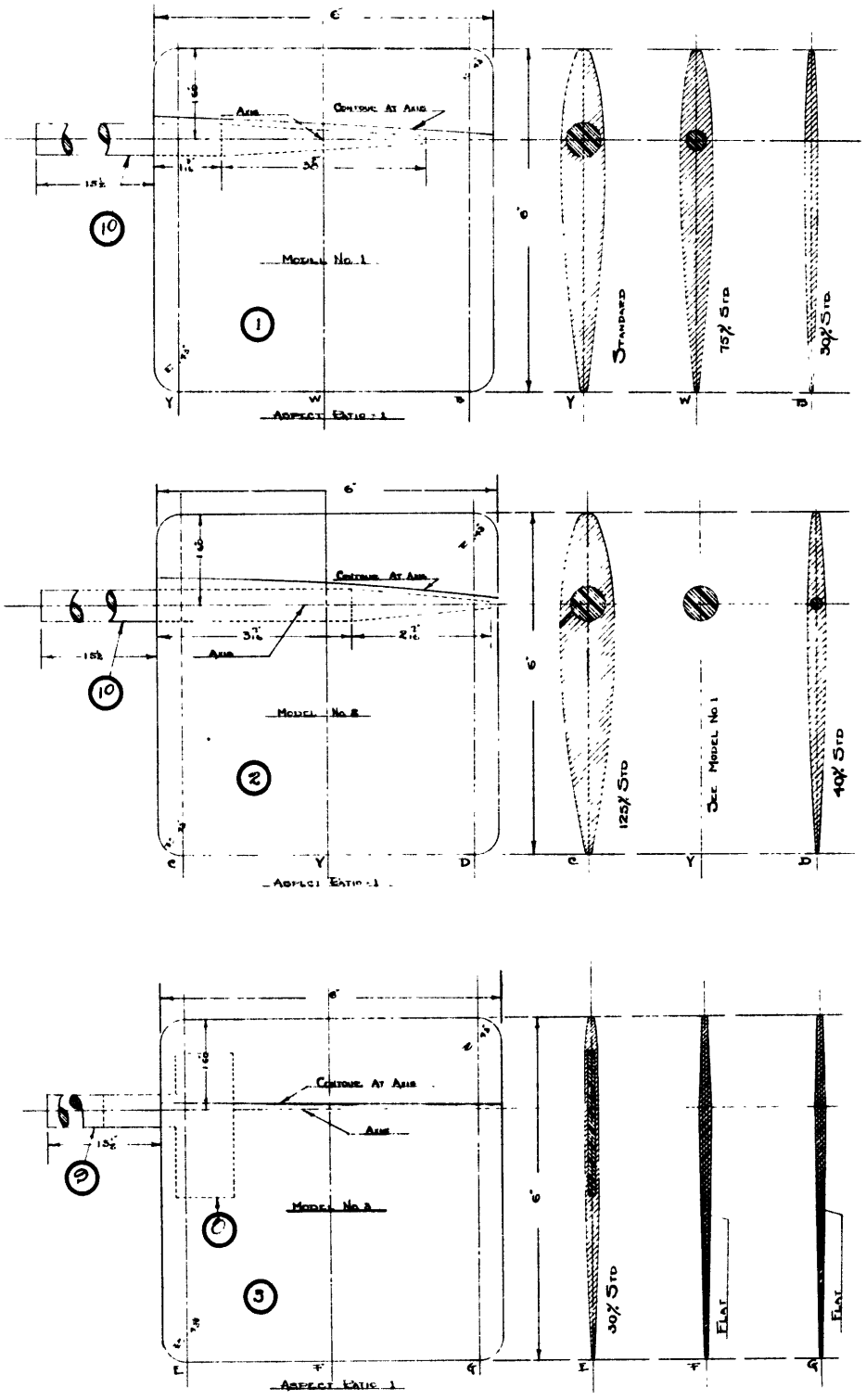

FIG. 5 RUDDERS 1 - 3

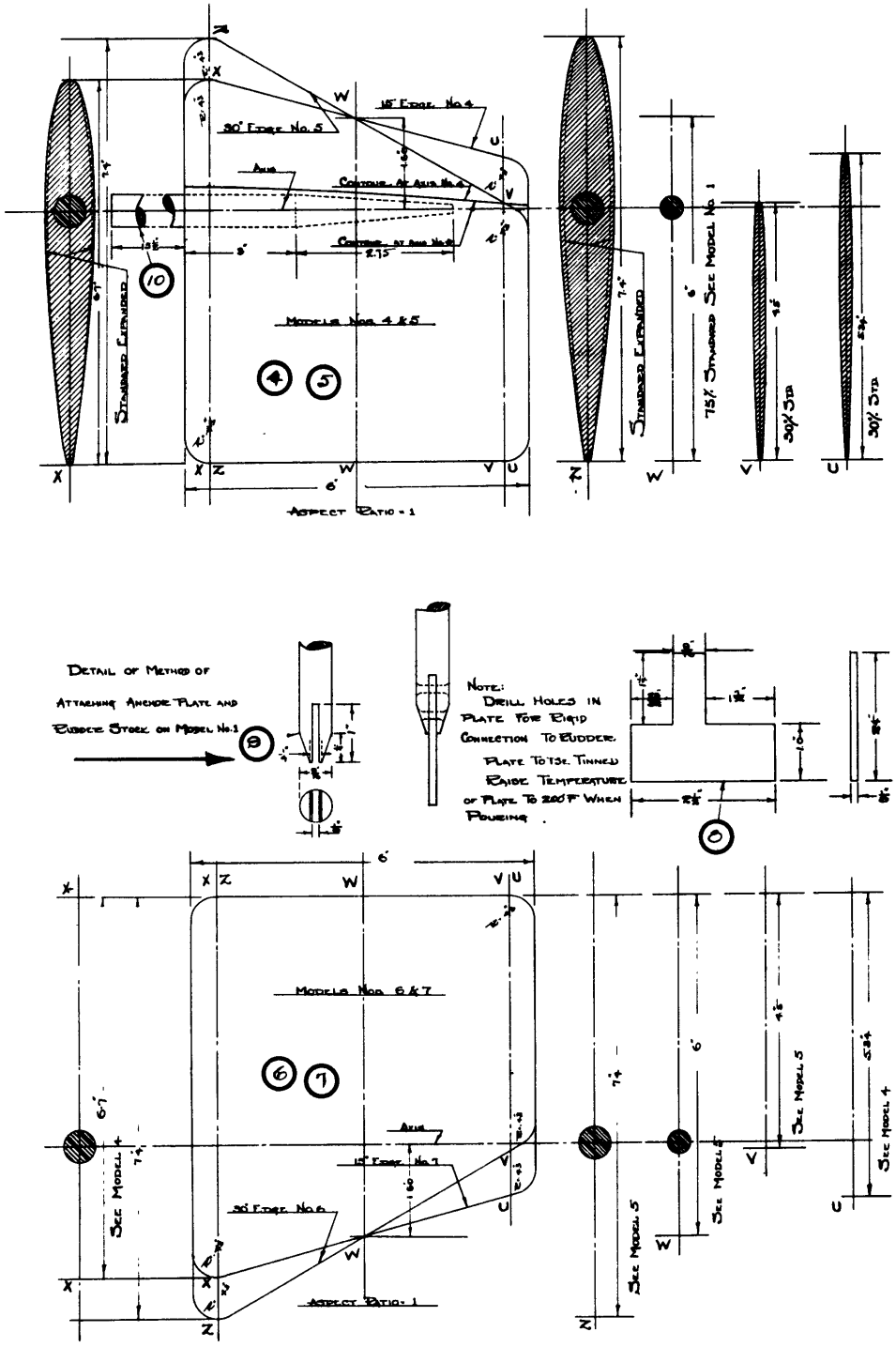

FIG. 6 RUDDERS 4 - 7

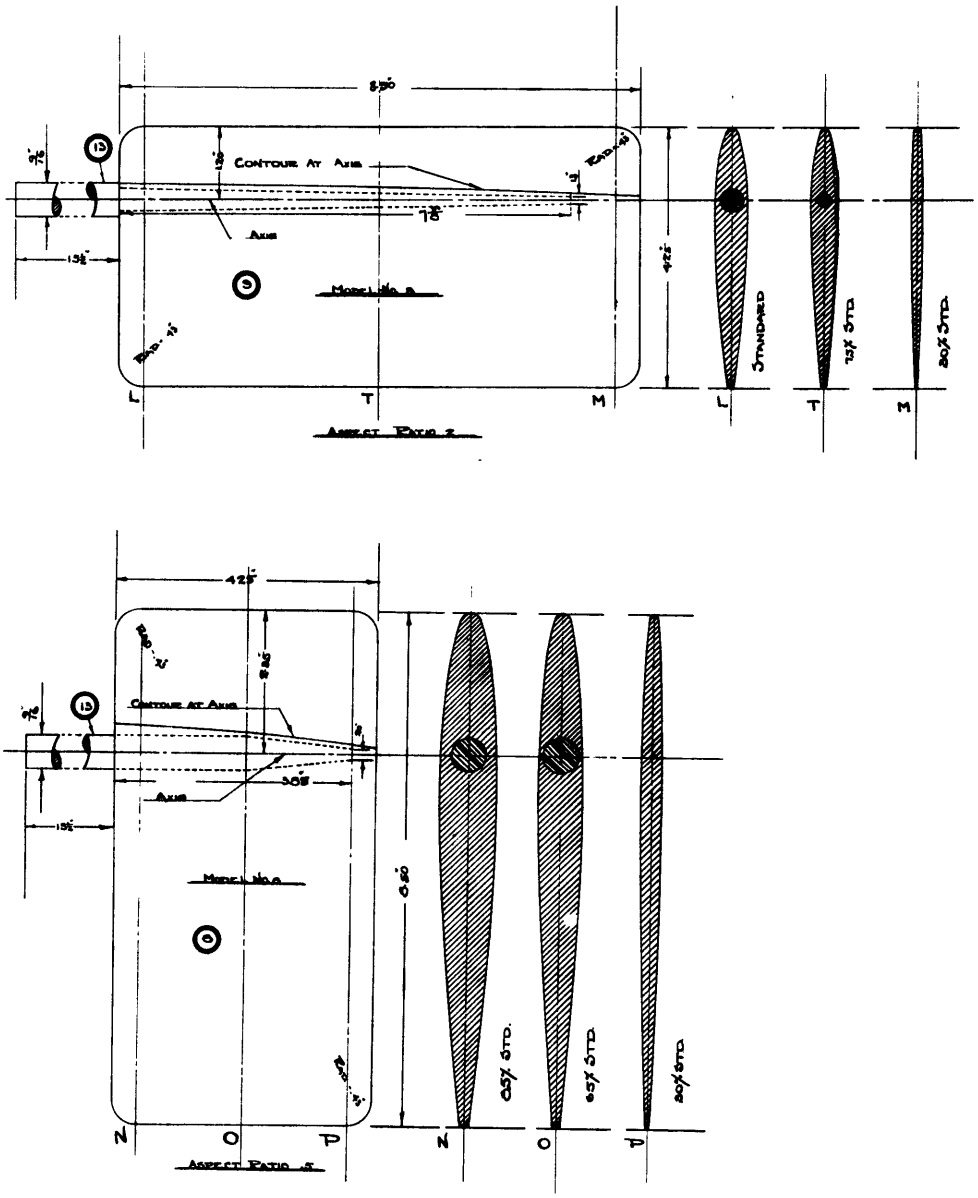

FIG. 7 RUDDERS 8 & 9

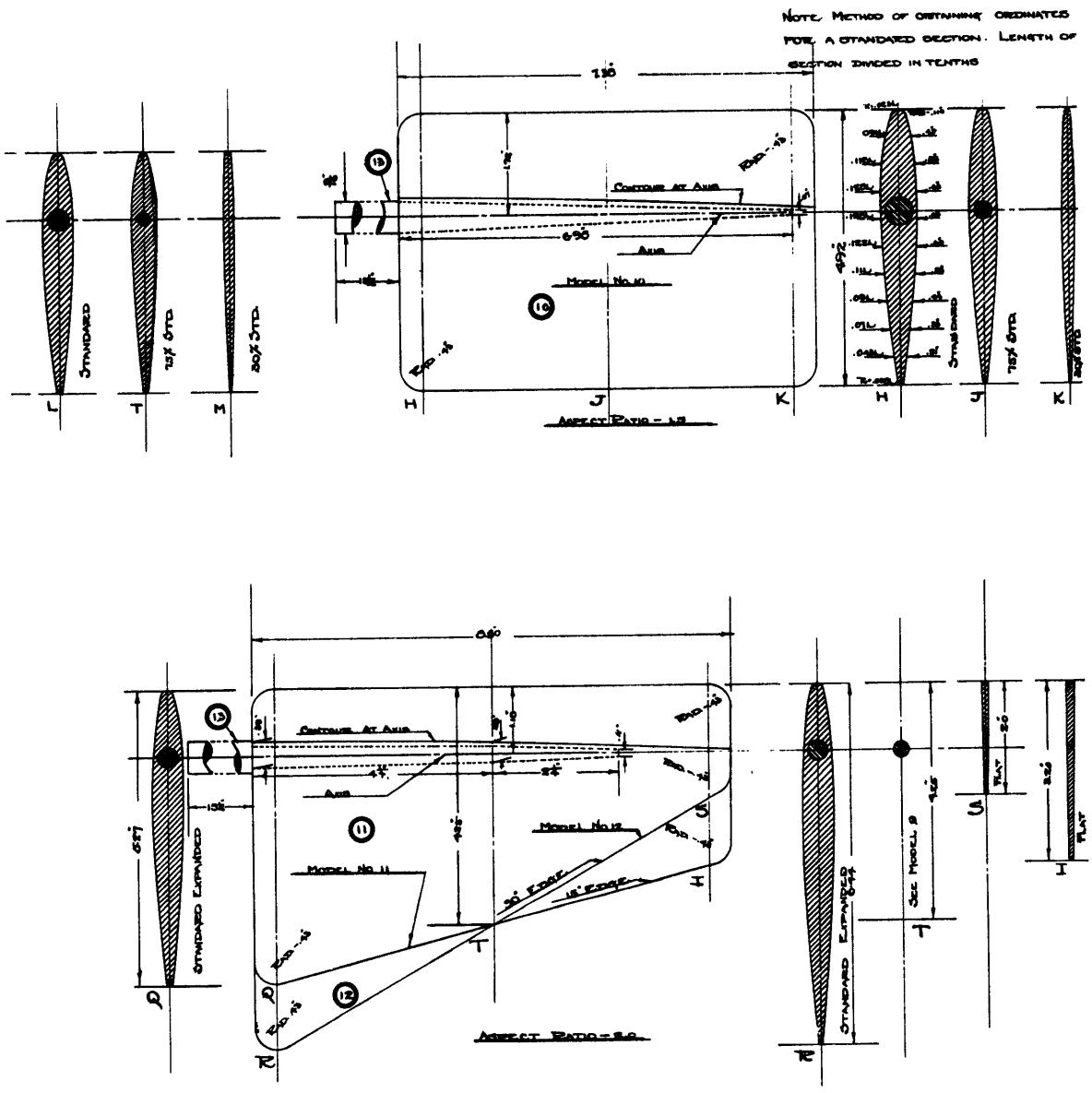

FIG. 8 RUDDERS 10 - 12

Effect of Neighboring Hull

From theoretical considerations it is at once obvious that for the condition of the rudder flush with the hull, the effective aspect ratio should be twice that of the rudder itself. A series of runs were made at 2.5 knots with hull clearances varying from 0" to 2" to determine at what clearance the influence of the hull became negligible. Although no runs were made at greater clearances than two inches, the data indicated that a further separation would have had little effect, Fig. 9. This two inch clearance corresponds to one-third of the span (or rudder depth) in the case of the rudder tested (aspect ratio = 1.0). However, for the rudders of aspect ratios 1.5 and 2.0, which have a larger span, the ratio of clearance to span would not be so great and the effect of the neighboring hull would perhaps be more appreciable. Unfortunately, the shortness of the rudder stock made the use of a clearance of more than two inches impossible.

Effect of Speed - Most Suitable Speed

A series of runs at different speeds varying from 1.5 to 3.0 knots showed that the highest speed at which the rudders could be run without considerable oscillation and irregularity of readings was 2.5 knots. This was chosen as the speed at which to run the complete test. The data taken on these runs at various speeds are plotted as lift coefficient and L/D in Fig. 10. A slight variation in the general character of the lift coefficient curves is evident, but the law of the dependence of lift upon the square of the speed is borne out by their good general agreement.

Correction for Wake

The wake of the float was determined by pitot tube measurements at various depths below the hull. The data are plotted as per cent of float speed against distance below hull, Fig. 11. Since the forces on the hydrofoil vary as the square of the velocity, all corrections for wake must be based upon the square of the wake. Thus, for a given distance below the hull, the correction will be determined by the wake-squared at that depth and also upon the chord (or rudder width) at that point. To find the correction for a non-tapered hydrofoil it is only necessary to run a planimeter over the curve of wake-squared between the abscissas corresponding to the depths of the upper and lower extremities of the hydrofoil. To determine the correction for the tapered hydrofoils it is necessary to take account of the variation of chord, or the distribution of area, with respect to the span and position in the wake. To accomplish this, the ordinates of the wake-squared curve, previously obtained, were multiplied by the ratio of the local value of the chord to the mean value. This gave a weighted wake-squared curve from which the wake correction was obtained by mechanical integration as before. A separate curve was necessary for each tapered rudder

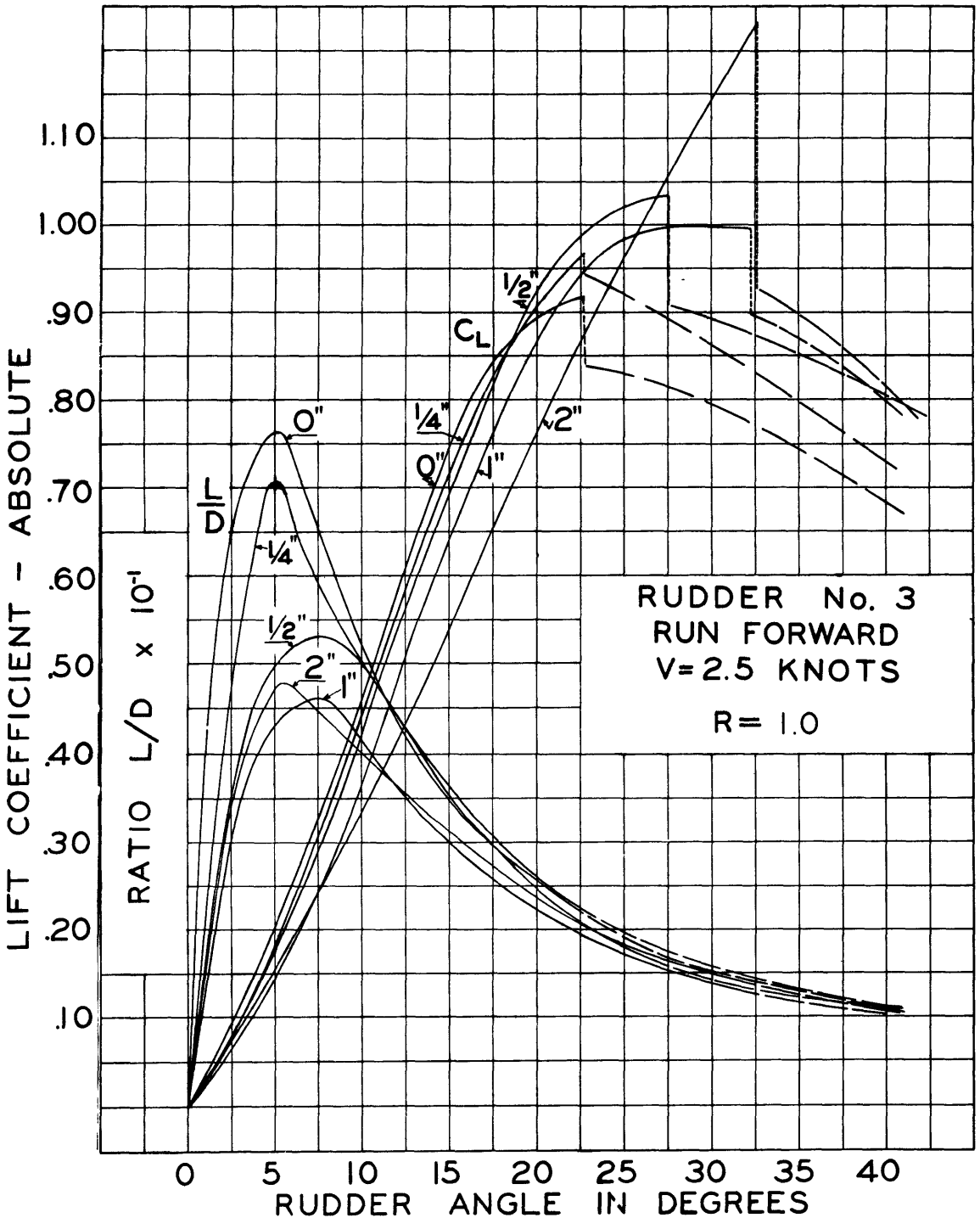

FIG. 9 EFFECT OF VARYING HULL CLEARANCE

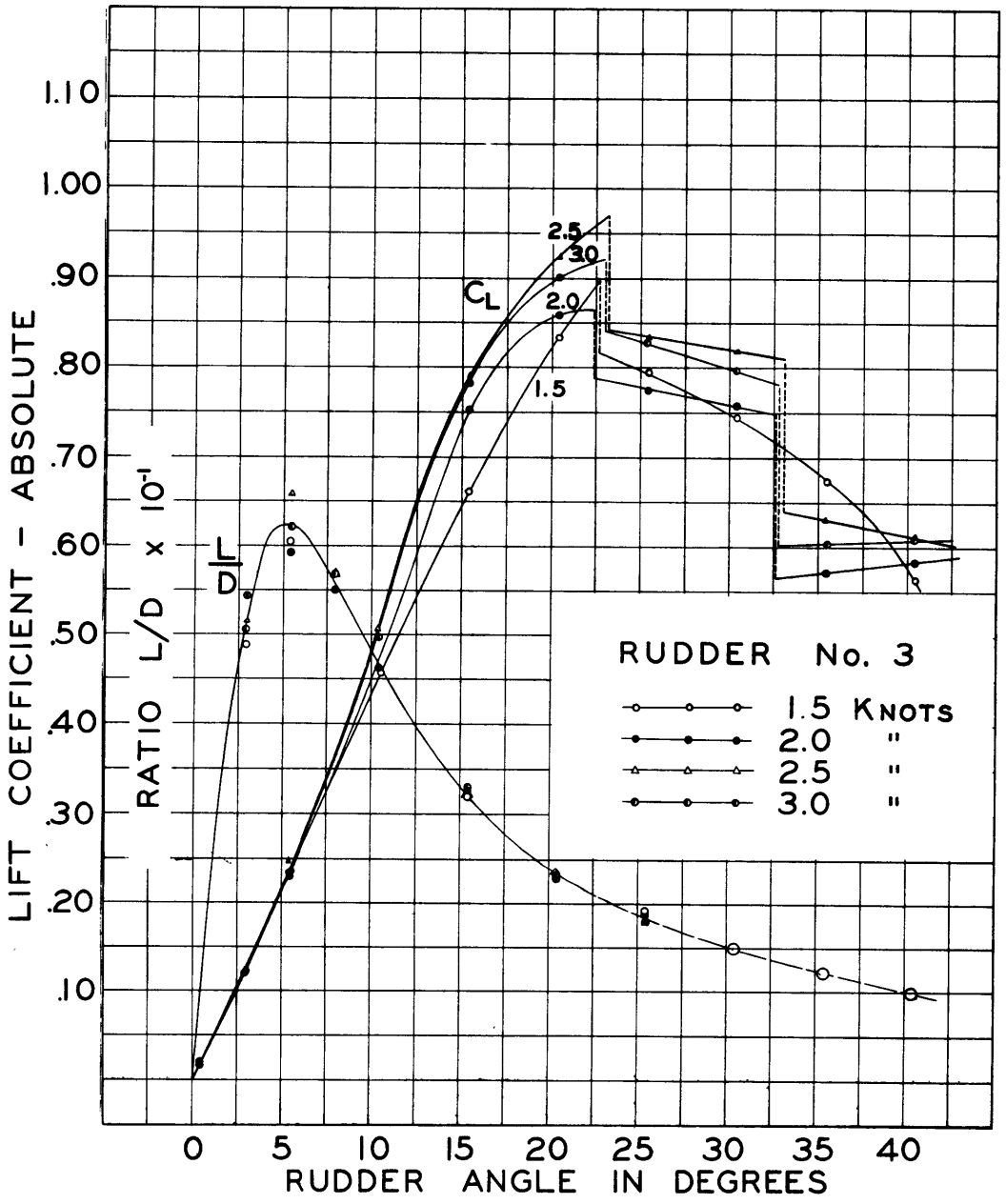

FIG. 10 INFLUENCE OF SPEED

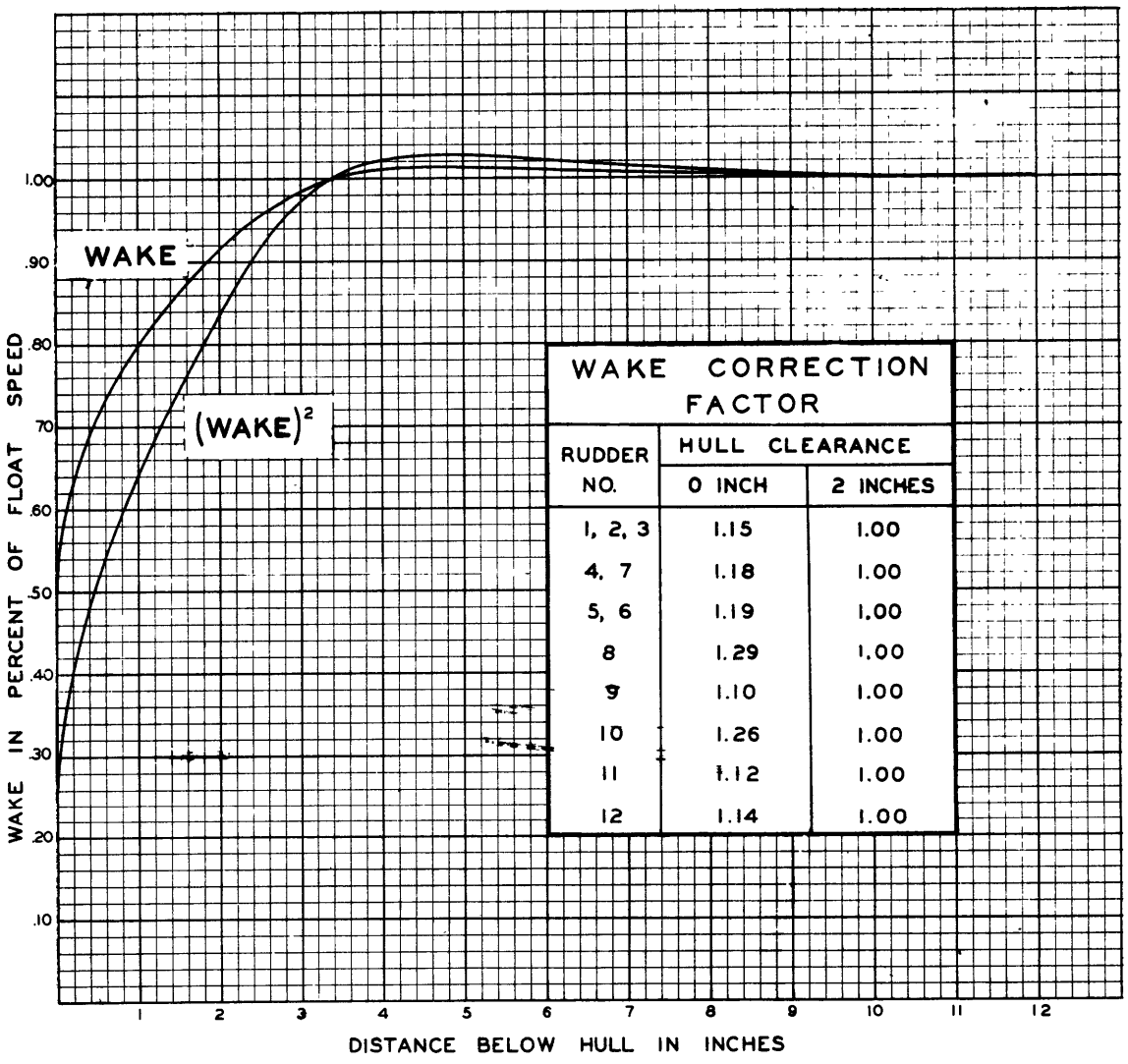

WAKE CORRECTION FACTOR

RUDDER NO.	HULL CLEARANCE	
	0 INCH	2 INCHES
1, 2, 3	1.15	1.00
4, 7	1.18	1.00
5, 6	1.19	1.00
8	1.29	1.00
9	1.10	1.00
10	1.26	1.00
11	1.12	1.00
12	1.14	1.00

FIG. 11 WAKE OF FLOAT

and for each condition of clearance.

IV REDUCTION of DATA

The data obtained in the tests, for convenience in plotting, were reduced to the form of absolute coefficients, namely–

Absolute coefficient of lift:

$$C_L = \frac{L}{\frac{1}{2}\rho A v^2}$$

Absolute coefficient of drag:

$$C_D = \frac{D}{\frac{1}{2}\rho A v^2}$$

Absolute coefficient of moment (about quarter–chord point):

$$C_{Mo} = \frac{Q}{\frac{1}{2}\rho c A v^2}$$

The center of pressure as per cent of chord from leading edge and L/D ratio were also calculated and plotted.

Center of Pressure

$$C.P. = \frac{100}{c}\left[d - \frac{Qm}{\sqrt{L^2 + D^2}\ \cos\psi}\right] \qquad (4)$$

Torque (about quarter–chord point)

$$Q = Qm\left[\frac{\frac{c}{100}\,C.P. - \frac{c}{4}}{d - \frac{c}{100} \times C.P.}\right] \qquad (5)$$

In which

L = measured lift in pounds
D = measured drag in pounds
Qm= measured torque (about rudder stock) in lb. in.
Q = torque about quarter–chord point in lb. in.
A = projected area of hydrofoil in sq. ft.
v = speed in ft. per sec.
ρ = density of water – poundals per cu. ft.
c = mean chord of hydrofoil in in.
d = distance from leading edge to center of rudder stock in in.
ψ = angle of the resultant $\sqrt{L^2 + D^2}$ with the normal of the hydrofoil. For angles of attack greater than 10°, ψ becomes so small that $\cos\psi = 1$ for all practical purposes.

Correction for Carriage Speed

Actually it was impossible to make every run at exactly 2.50 knots; the speed of the carriage as determined by a chronograph arrangement varied from 2.40 to 2.60. The following formulae make correction for this and give the actual forces in pounds and torque in pound inches for a true speed of 2.50 knots:

$$L = (G_2 - G_4)\left(\frac{2.50}{v_c}\right)^2 \times K F \qquad (6)$$

$$D = (G_1 - G_3)\left(\frac{2.50}{v_c}\right)^2 \times K F \qquad (7)$$

$$Q_m = (1.94\, G_1 - 2.17\, G_2 + 3.80\, G_3 - 3.04\, G_4)\left(\frac{2.50}{v_c}\right)^2 K F_Q \qquad (8)$$

In which

K = wake correction factor
F = dynamometer calibration factor for lift and drag
F_Q = dynamometer calibration factor for torque
v_c = actual carriage speed for run

G_1, G_2, G_3, and G_4 are the dynamometer dial gage readings. The numerical constants appearing in Eq. (8) are the moment arms measured from the rudder stock center for the forces represented by the corresponding dial gage readings.

Center of Pressure at Zero Angle

Although it is not necessary for purposes of rudder design that the center of pressure at zero angle of attack be known since the torque vanishes at this position, nevertheless, a value at 0° on the center of pressure curve would permit a more accurate drawing of the curve since the data for angles of attack are not as accurate as might be desired. This is due to constant errors in comparatively small measured values of the forces and torques, which may combine in the calculation in such a manner as to be additive and to give large errors in the result. For this reason the spots on the center of pressure curve for 10° or less should not be regarded as necessarily indicating the true position of the curve.

The position of the center of pressure measured from the center of the rudder stock is given by the ratio

$$\frac{Q_m}{\sqrt{L^2 + D^2}\ \cos\psi} \qquad (9)$$

however at 0° the torque Q_m vanishes as does the lift L. The only force acting

is the drag which passes through the rudder stock center and is parallel to the chord. Consequently the ratio given above reduces to the indeterminate form of 0/0.

For small angles of attack Eq. (9) may be written with good approximation as simply Q_m/L, which, though indeterminate, may be easily evaluated by differentiating both numerator and denominator with respect to α, the angle of attack. This gives

$$C.P._s = \frac{\frac{dQ_m}{d\alpha}}{\frac{dL}{d\alpha}} \qquad (10)$$

The numerator in Eq. (10) is but the slope of the Q_m curve plotted against angle of attack, and similarly the denominator is the slope of the lift curve plotted against α. These slopes can be measured from the plotted curves in the region of $\alpha = 0°$, and the position of the center of pressure determined from their ratio. This is possible only for the case of the rudders run reversed as when the rudder is run with the leading edge forward the center of pressure at small angles lies very near the position of the rudder stock center and the measured torque is consequently so small that all accuracy is lost.

Correction for Rudder Stock

The C_D values obtained for rudders run at two inch hull clearance were corrected for the drag of the two inch length of rudder stock exposed above the rudder. This correction, however, amounted to approximately 0.007.

V DISCUSSION of RESULTS

The hydrodynamic characteristics of the twelve hydrofoils tested are given for the four test conditions in Figs. 12-23, inclusive. Curves of C_L, C_D, C_{Mo}, L/D, and C.P. plotted against angle of attack are shown. A resume of the characteristics of these curves appears in Tables I and II; Table I being for 2 inch hull clearance and Table II for 0 inch hull clearance. The thickness ratio given is that for the mid-span section.

For the sake of easy comparison of all rudders of aspect ratio 1, the curves of C_L and L/D are plotted for rudders 1-7 in Fig. 24 for the condition of zero clearance and for the rudder run forward. Similarly, these curves are given for rudders 9, 11, and 12 (R = 2) in Fig. 25.

The variation of C_L and L/D, with aspect ratio, is shown in Fig. 26 in which curves for aspect ratios 0.5, 1.0, 1.5, and 2.0 are given. Fig. 27 shows the effect of the aspect ratio upon the slope of the C_L-curve. Here are given only the data for the condition of 2 inch hull clearance, in which case the geometric and effective aspect ratios are identical.

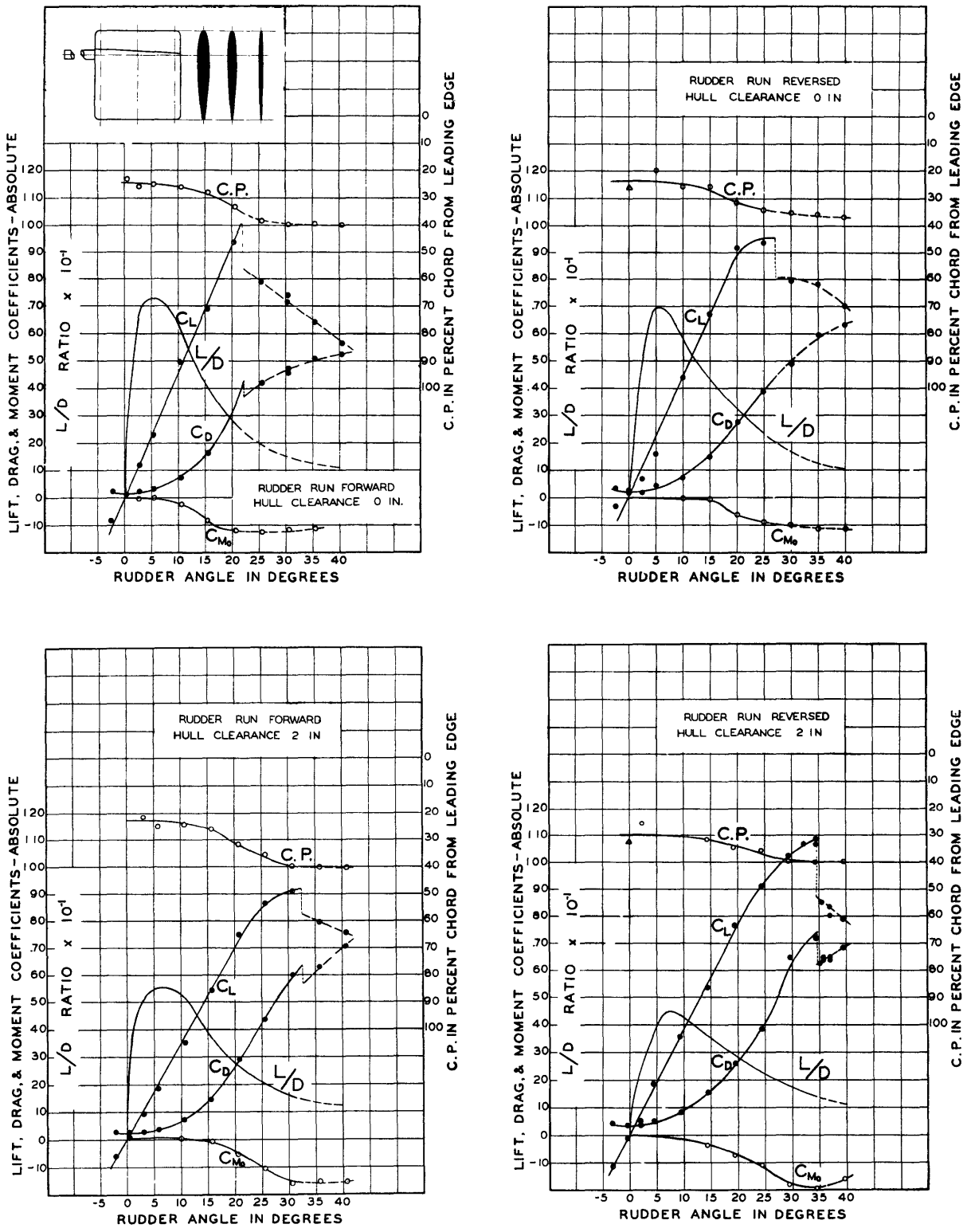

FIG. 12 RUDDER NO. 1 R = 1

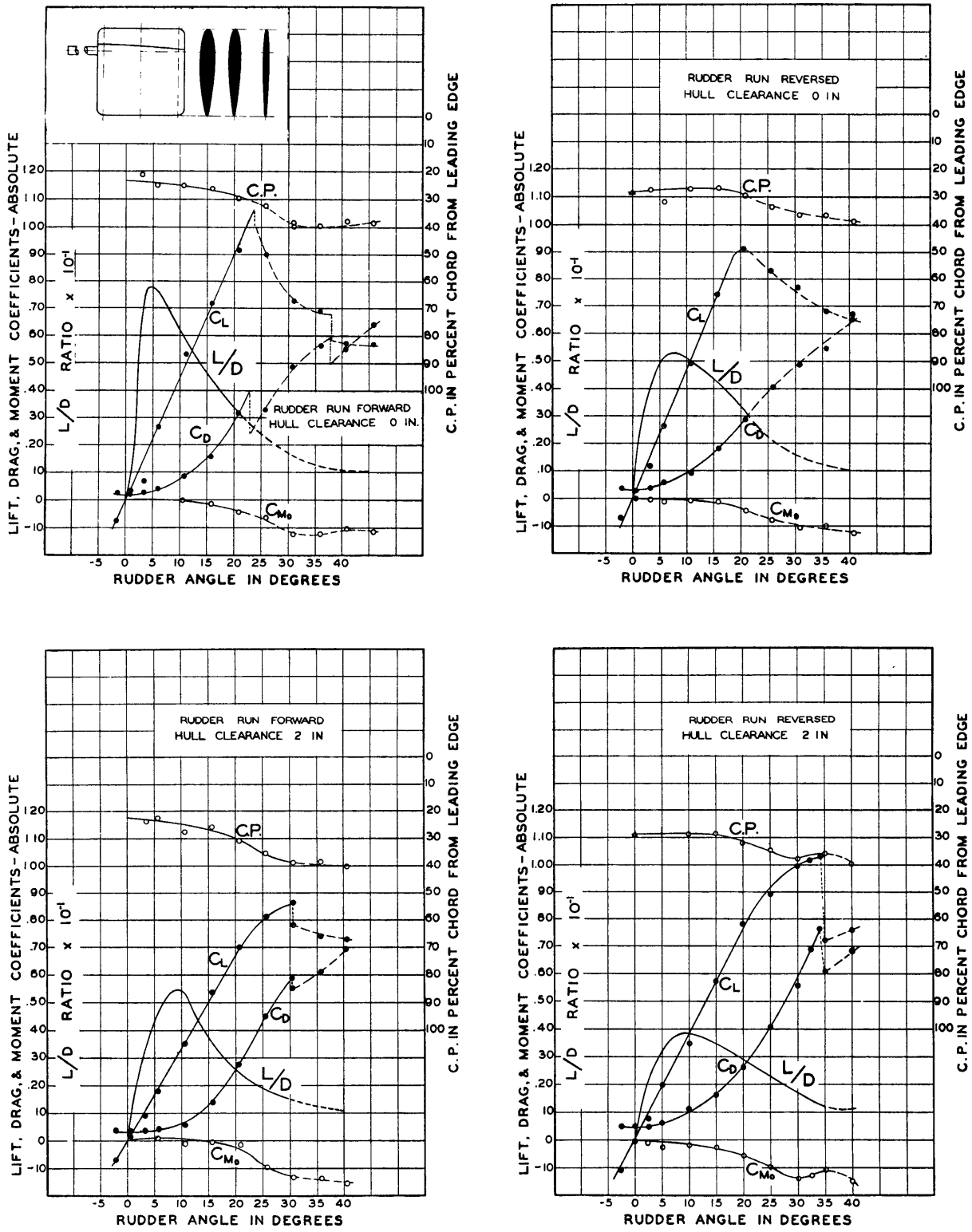

FIG. 13 RUDDER NO. 2 R = 1

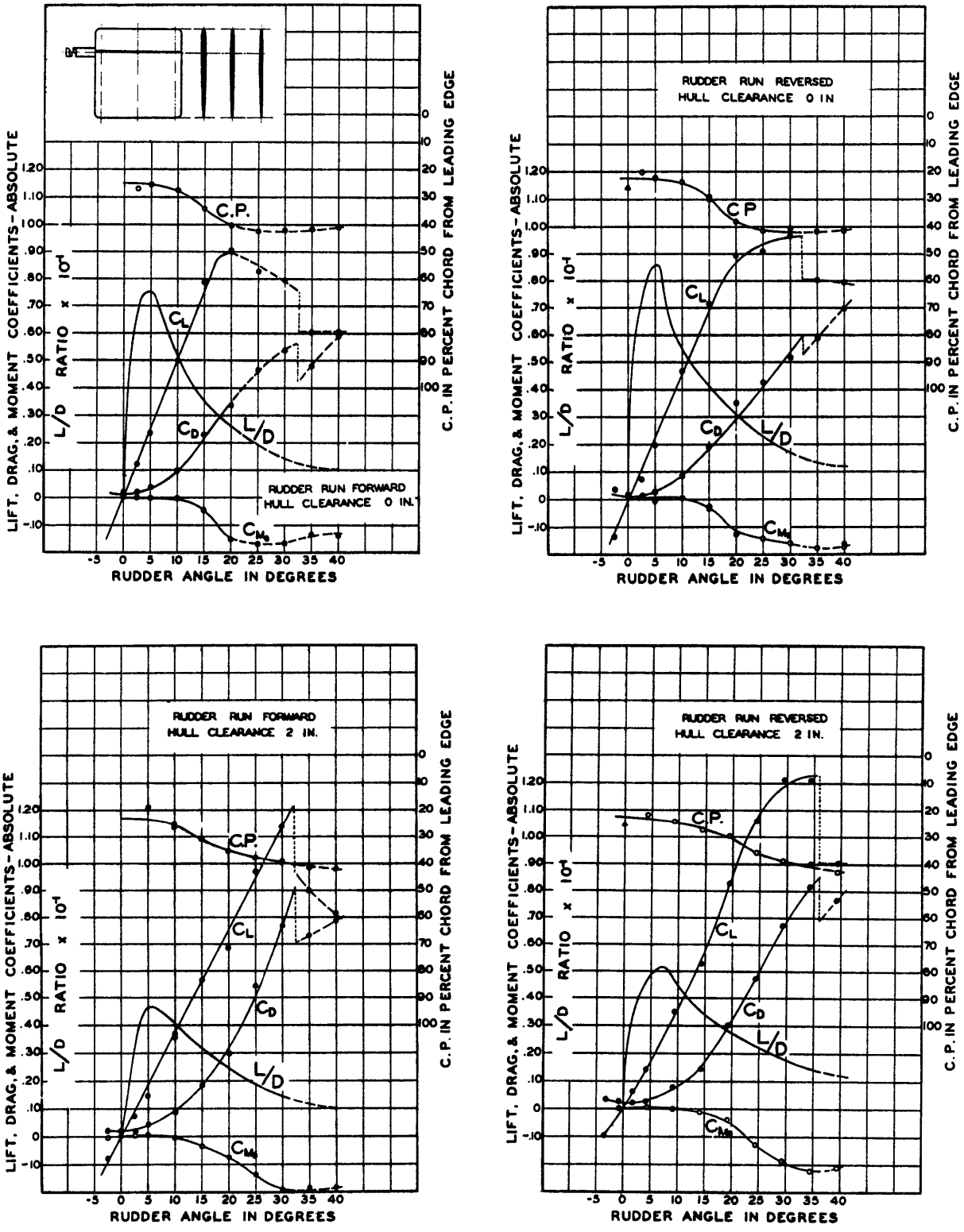

FIG. 14 RUDDER NO. 3 R = 1

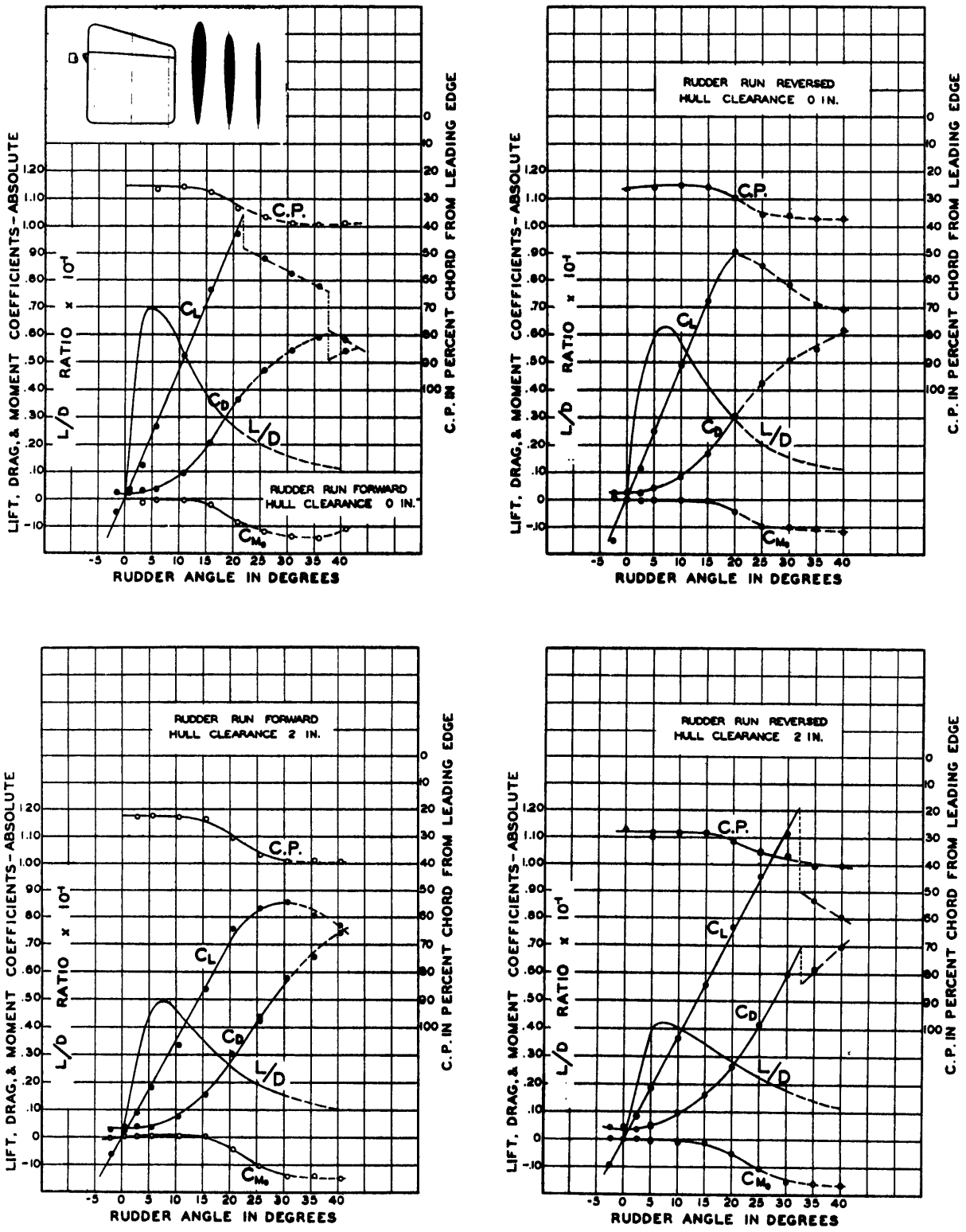

FIG. 15 RUDDER NO. 4 R = 1

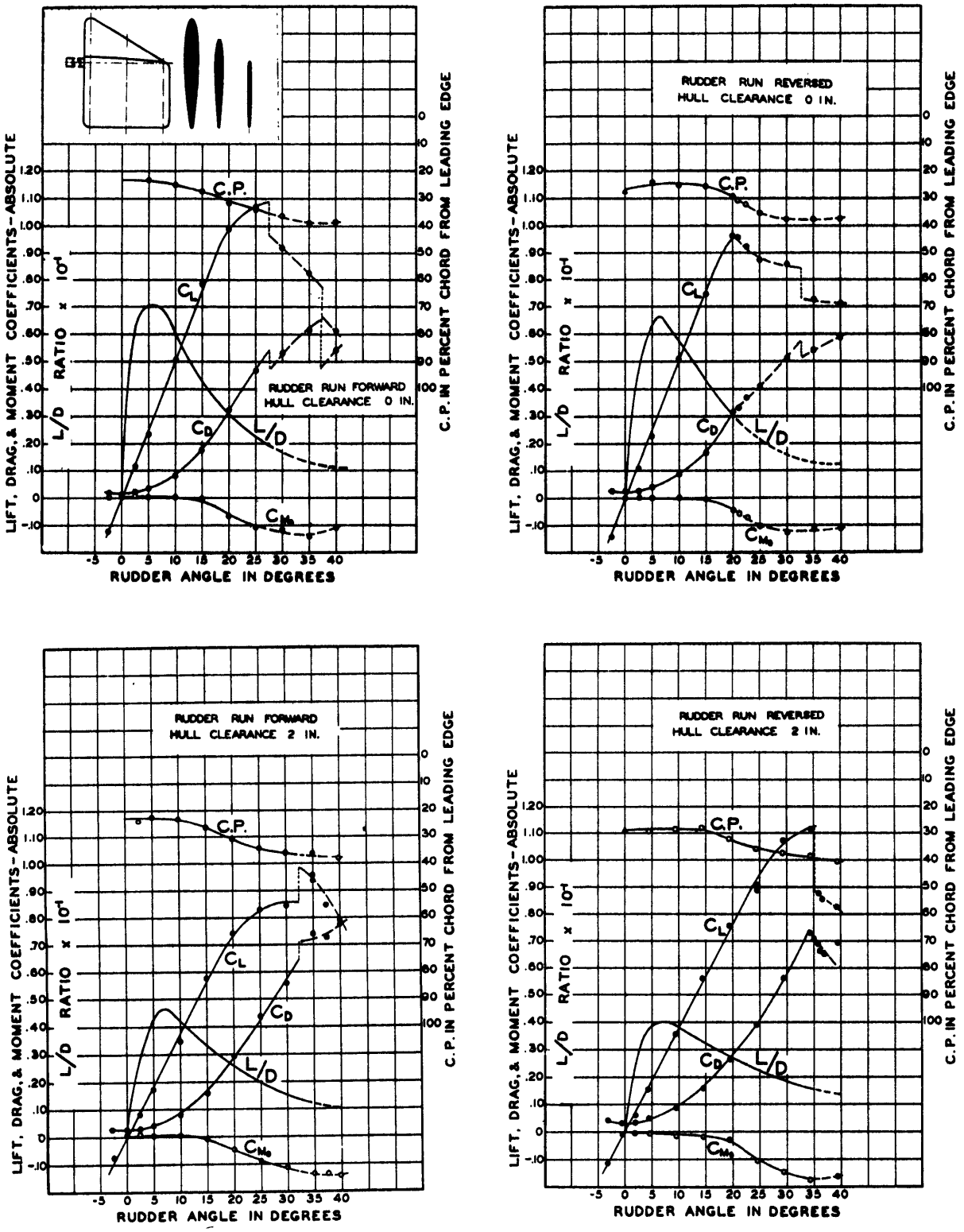

FIG. 16 RUDDER NO. 5 R = 1

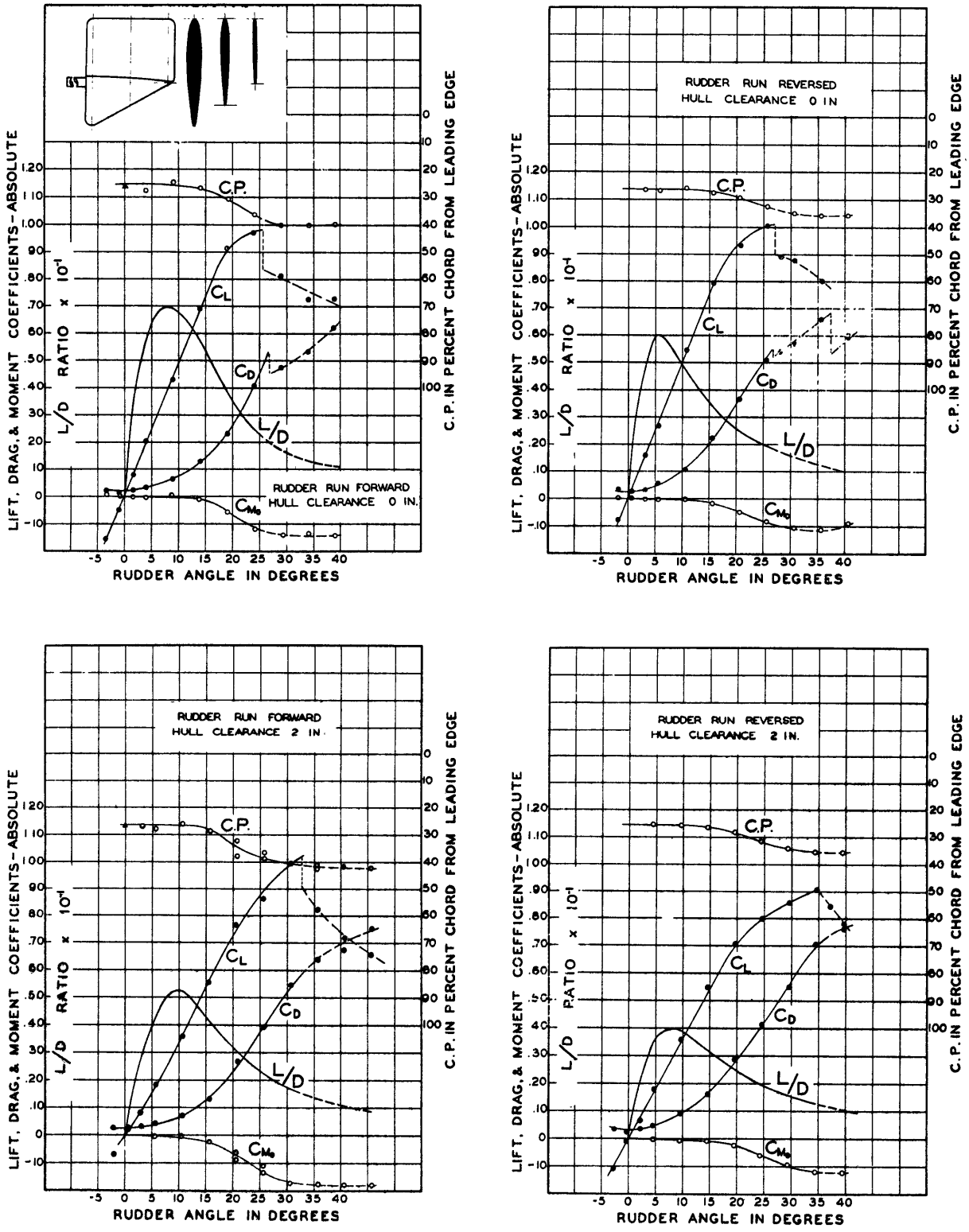

FIG. 17 RUDDER NO. 6 R = 1

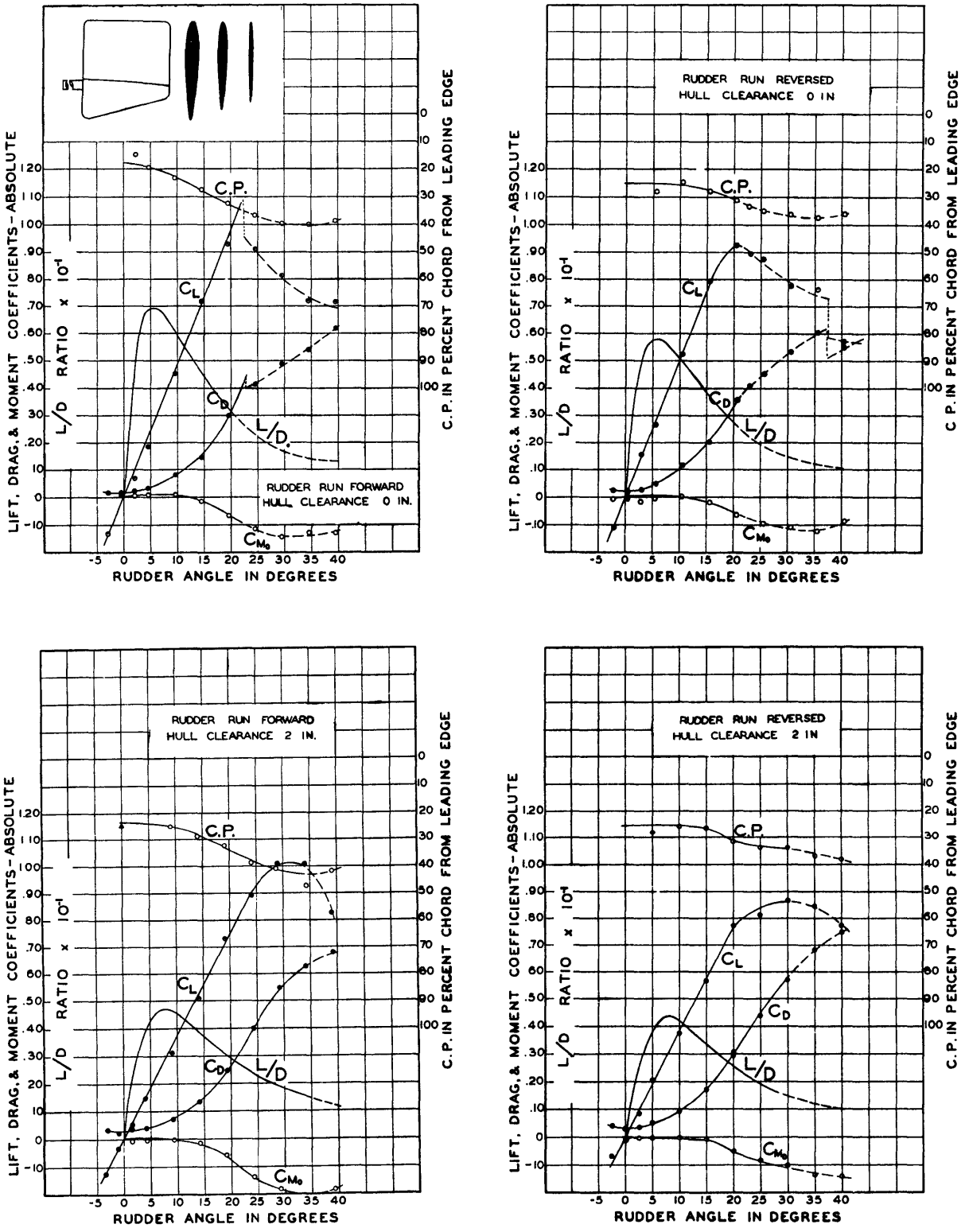

FIG. 18 RUDDER NO. 7 R = 1

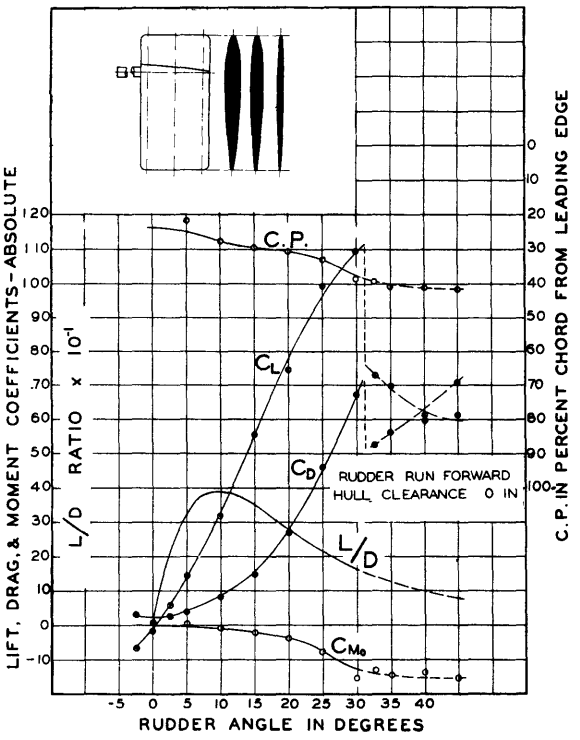

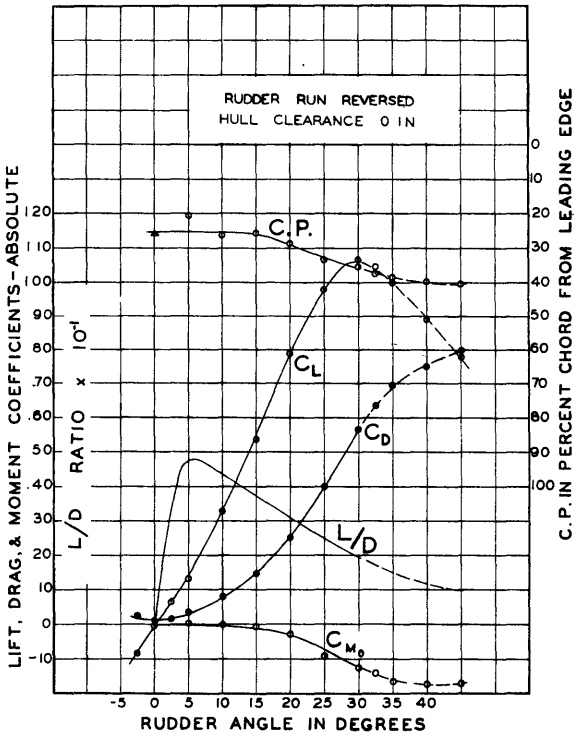

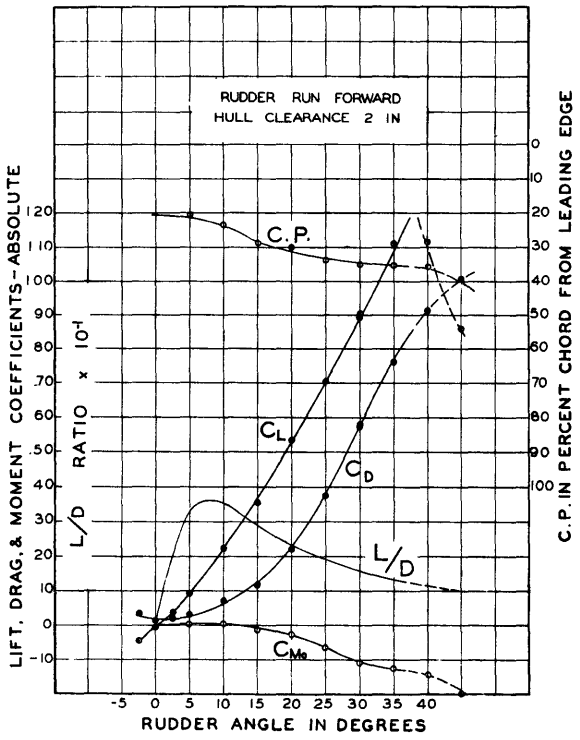

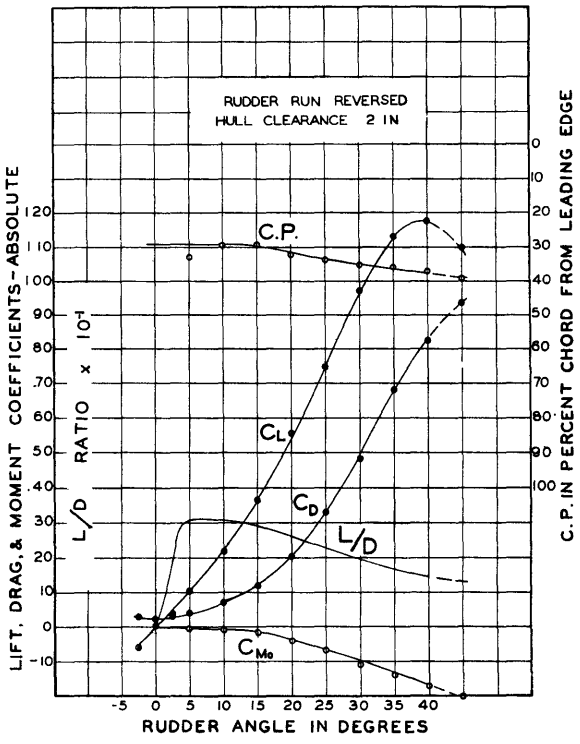

FIG. 19 RUDDER NO. 8 R = 0.5

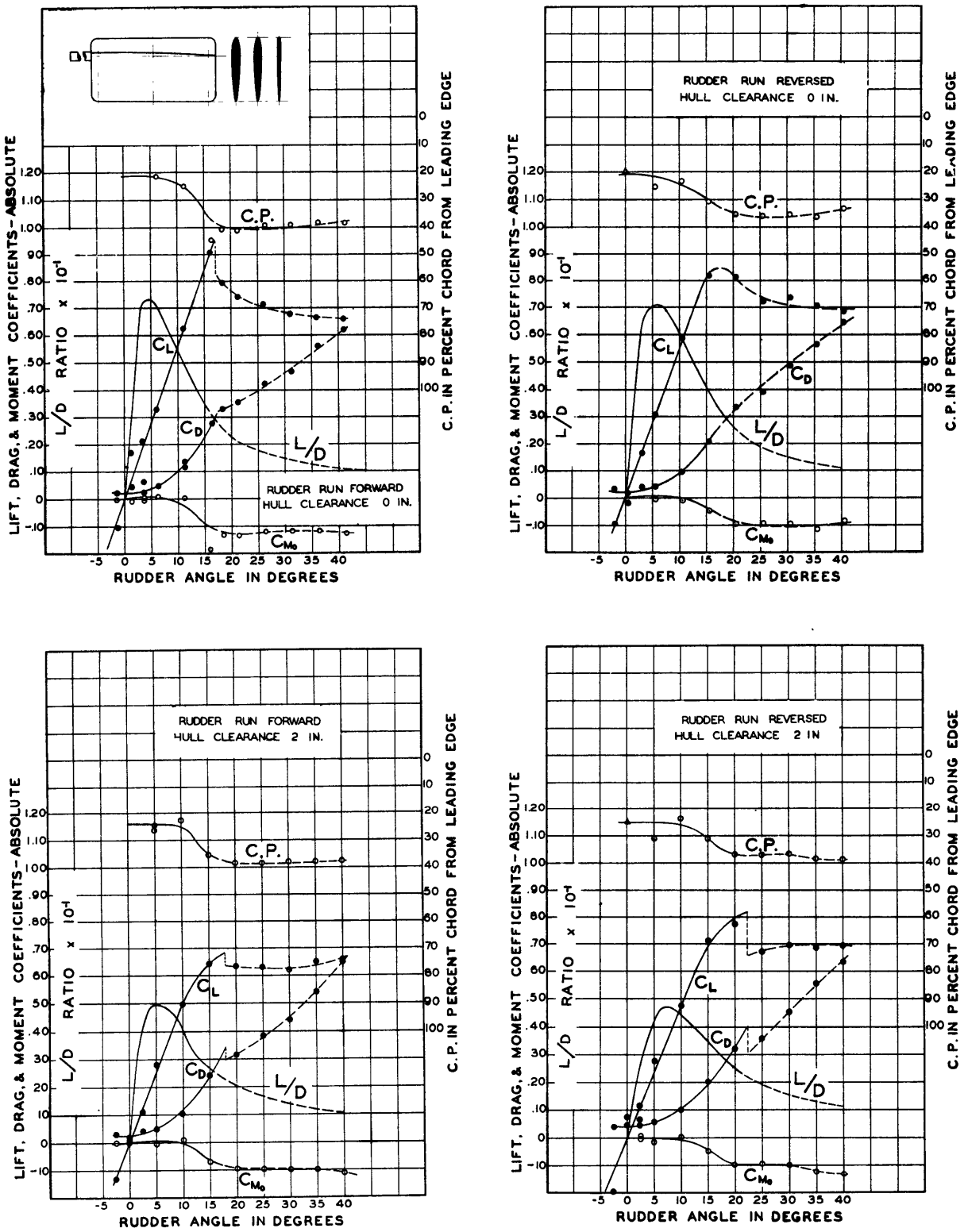

FIG. 20 RUDDER NO. 9 R = 2

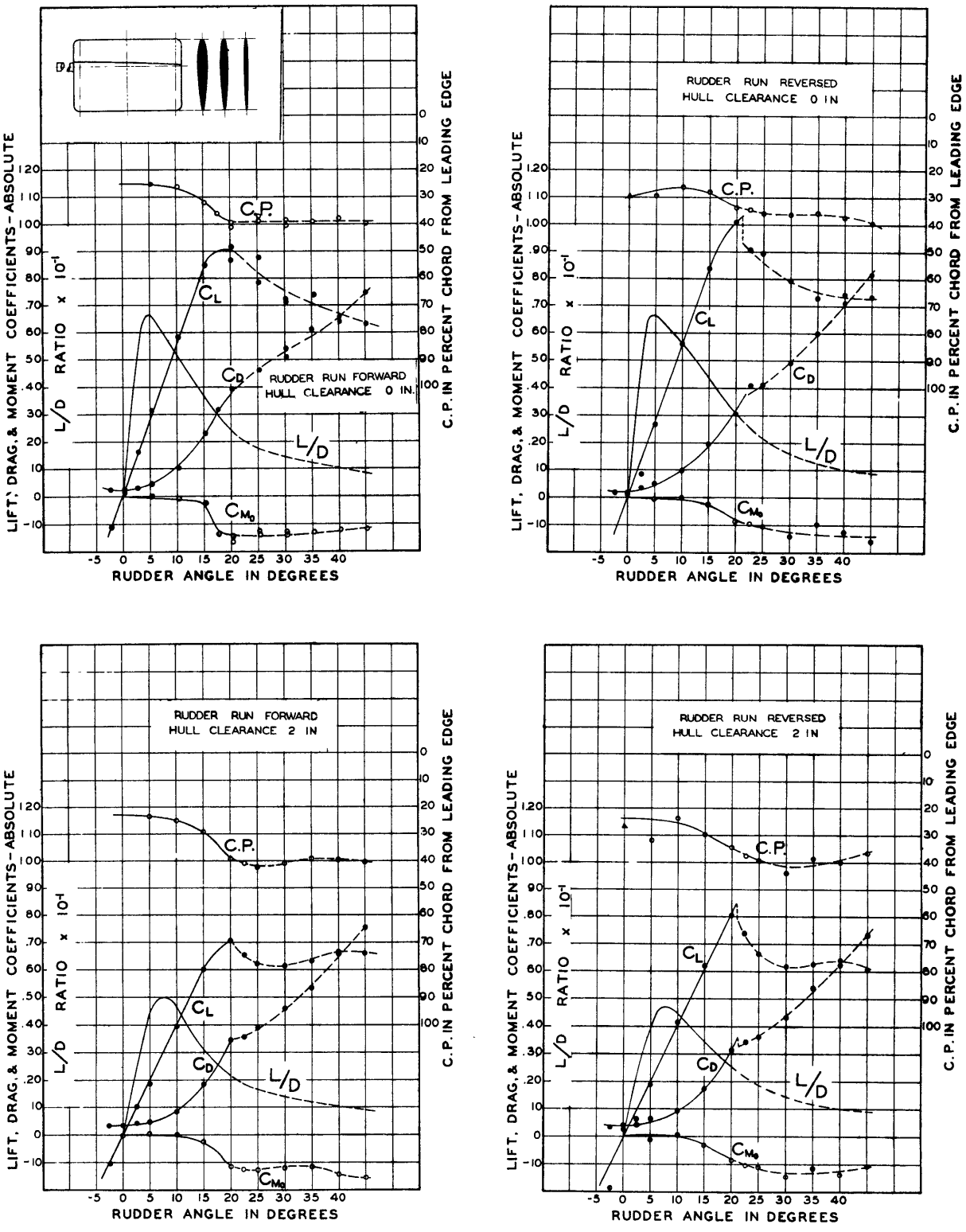

FIG. 21 RUDDER NO. 10 R = 1.5

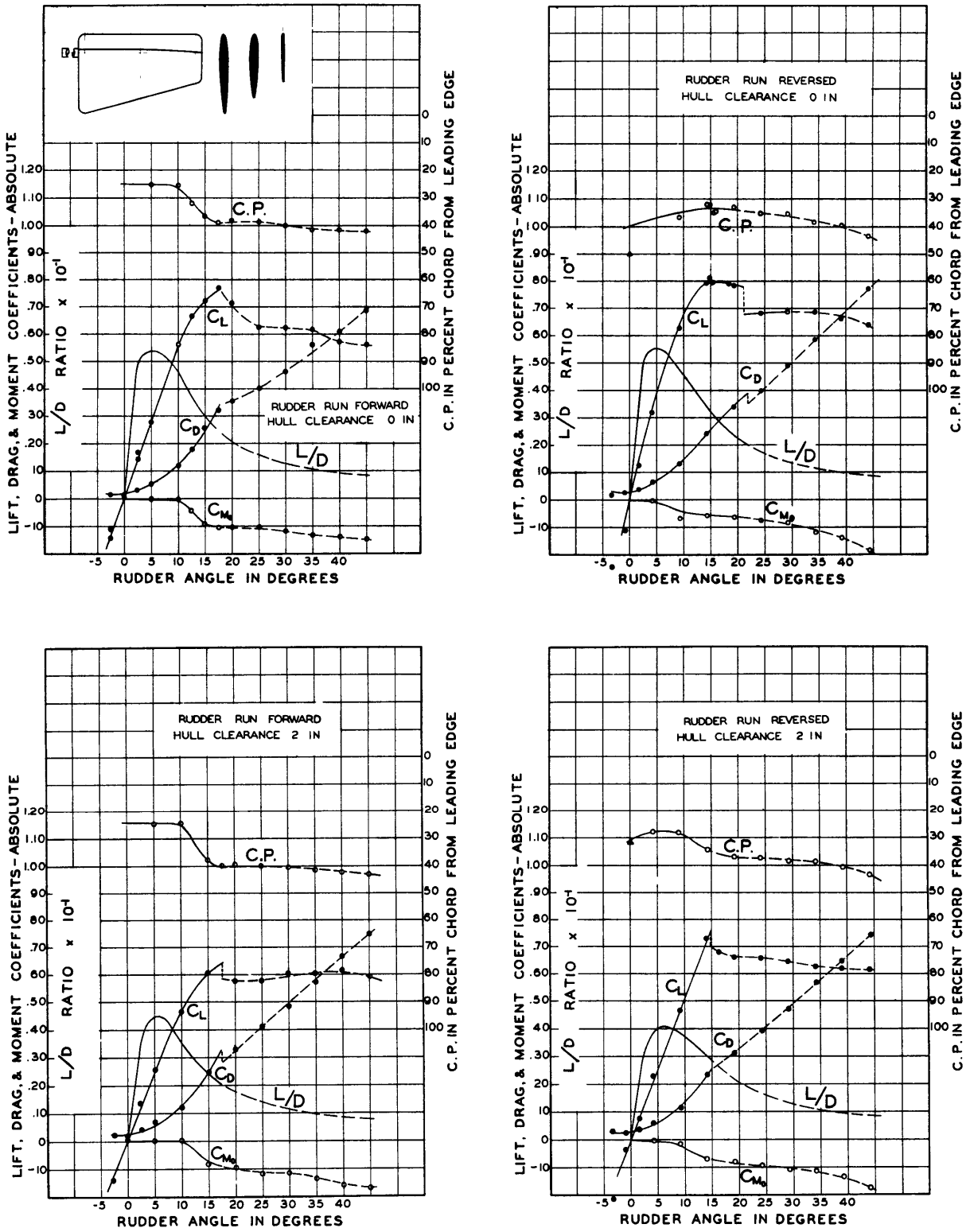

FIG. 22 RUDDER NO. 11 R = 2

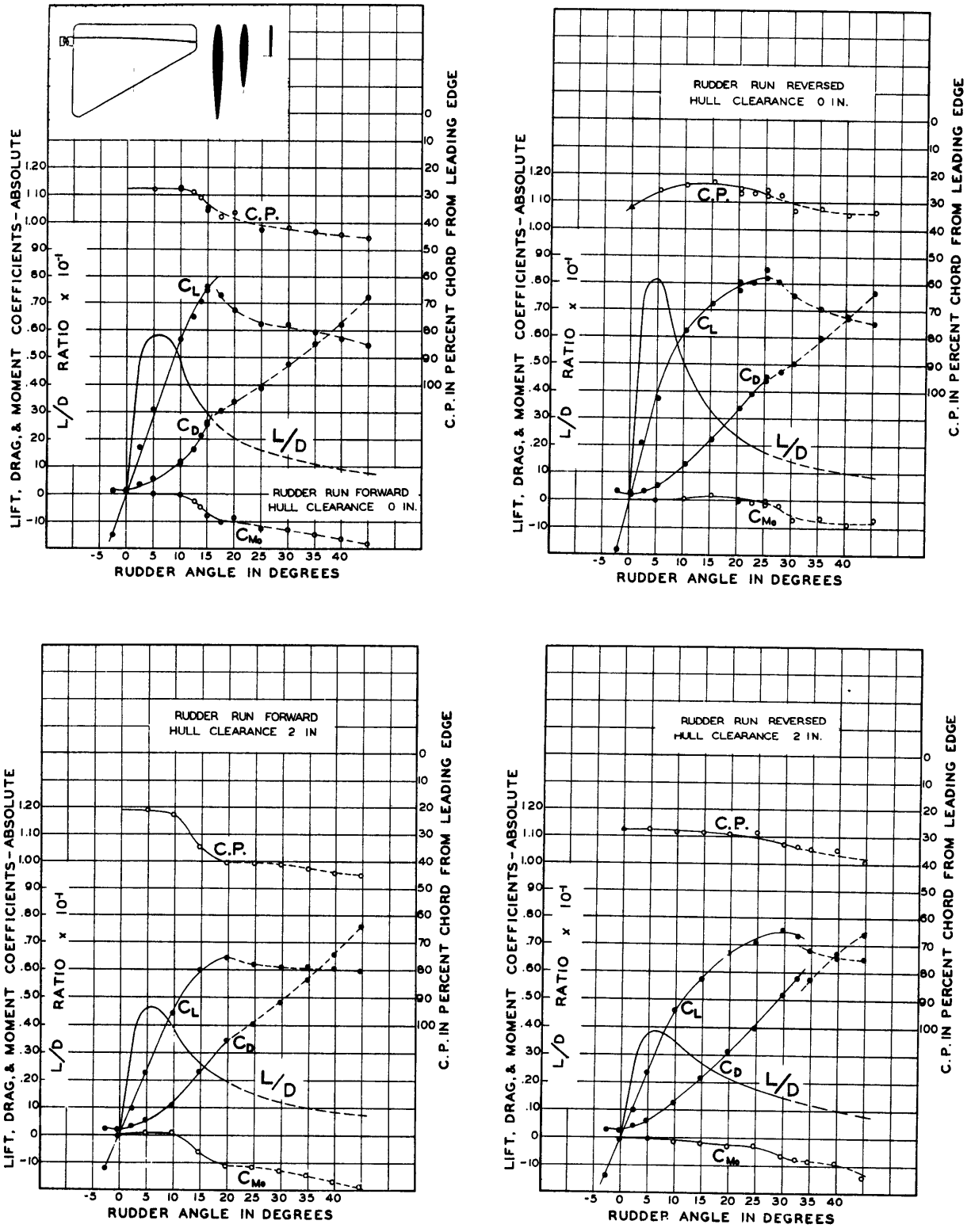

FIG. 23 RUDDER NO. 12 R = 2

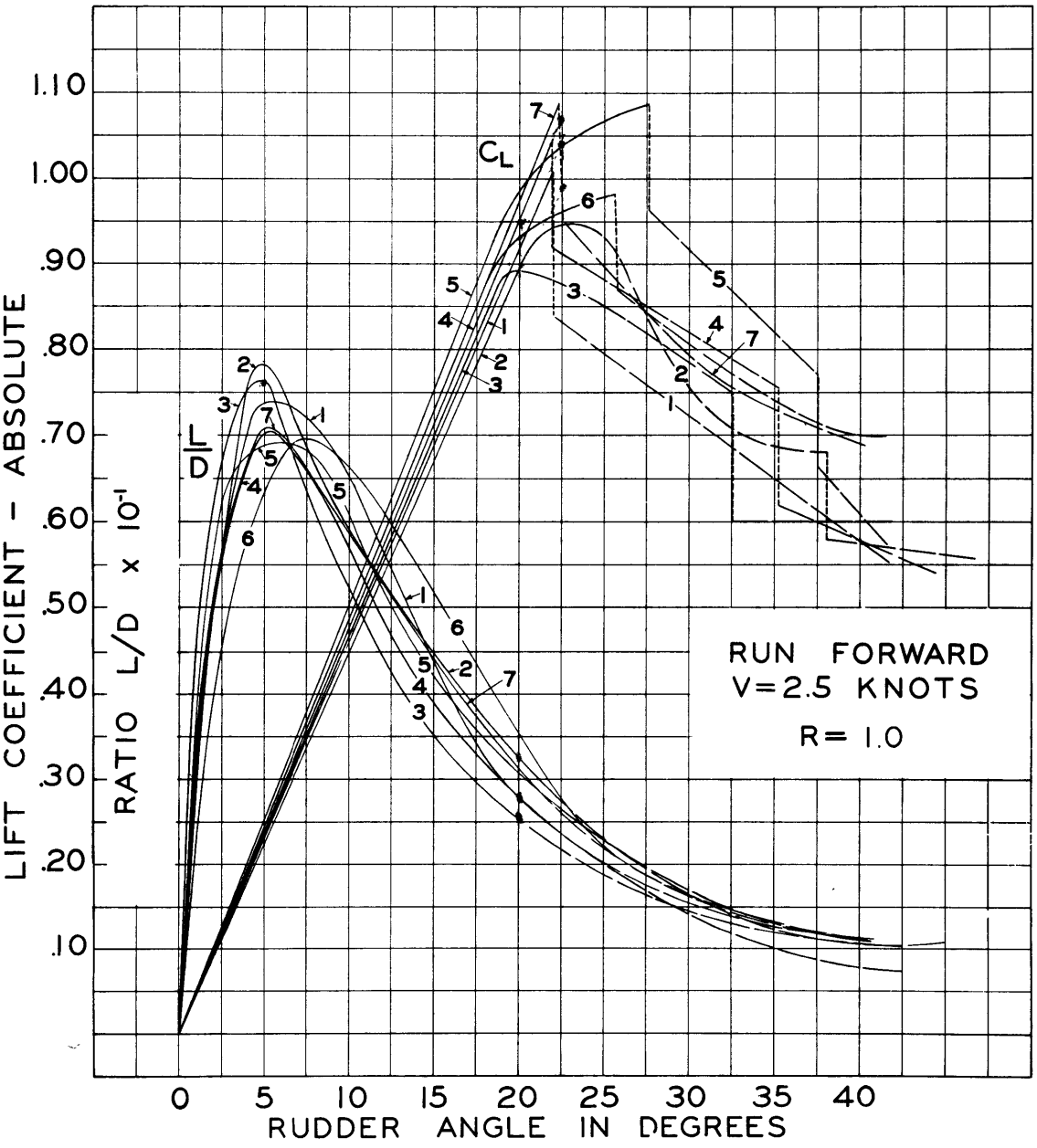

FIG. 24 RUDDERS 1-7.

TABLE I

Rudder No.	Aspect Ratio	Thickness Ratio	Slope C_L-Curve	$C_{L_{max}}$	Burble Point	L/D for $C_L = .75$	$\frac{c \cdot C_{Mo}}{C_{L_{\alpha=30°}}}$
2" CLEARANCE — RUDDER RUN FORWARD							
8	0.5	.083	.0225	1.17	38°	1.80	.0830
3	1.0	.040	.0375	1.20	32°	2.45	.0835
1	1.0	.096	.0350	.92	32°	2.60	.0855
2	1.0	.128	.0335	.86	31°	2.20	.0725
4	1.0	.096	.0355	.85	31°	2.35	.0790
5	1.0	.096	.0375	.85	32°	2.50	.0705
7	1.0	.096	.0377	1.02	32°	2.85	.0925
6	1.0	.096	.0335	1.02	32°	3.00	.0840
10	1.5	.096	.0402	.70	20°	2.20*	.0783
9	2.0	.096	.0500	.68	18°	2.30*	.0545
11	2.0	.096	.0470	.64	17°	2.00*	.0710
12	2.5	.096	.0465	.64	20°	2.00*	.0745
2" CLEARANCE — RUDDER RUN REVERSED							
8	0.5	.083	.0230	1.17	38°	2.30	.0708
3	1.0	.040	.0360	1.23	36°	3.00	.0820
1	1.0	.096	.0385	1.08	34°	2.90	.0875
2	1.0	.128	.0385	1.03	34°	2.95	.0700
4	1.0	.096	.0370	1.20	32°	2.80	.0625
5	1.0	.096	.0380	1.12	35°	2.70	.0700
7	1.0	.096	.0385	.87	30°	2.60	.0650
6	1.0	.096	.0360	.91	34°	2.25	.0509
10	1.5	.096	.0405	.84	22°	2.80	.0860
9	2.0	.096	.0475	.82	22°	2.95	.0513
11	2.0	.096	.0510	.75	15°	2.55	.0570
12	2.0	.096	.0475	.75	32°	1.50	.0301

*For $C_{L_{max}}$.

TABLE II

0" CLEARANCE — RUDDER RUN FORWARD

Rudder No.	Aspect Ratio	Thickness Ratio	Slope C_L-Curve	$C_{L_{max}}$	Burble Point	L/D for C_L = .75	$\frac{c \cdot C_{Mo}}{C_L}$ $\alpha = 30^\circ$	Effective Aspect Ratio
8	0.5	.083	.0330	1.12	32°	2.85	.0800	.94
3	1.0	.040	.0507	.90	20°	3.50	.1045	2.07
1	1.0	.096	.0460	1.00	22°	3.80	.0870	1.70
2	1.0	.128	.0447	1.05	23°	4.20	.0765	1.60
4	1.0	.096	.0480	1.05	22°	3.65	.0810	1.84
5	1.0	.096	.0500	1.09	27°	4.35	.0680	2.00
7	1.0	.096	.0487	1.08	22°	4.30	.0885	1.90
6	1.0	.096	.0490	.98	27°	5.25	.0880	1.92
10	1.5	.096	.0565	.91	19°	4.10	.0775	2.67
9	2.0	.096	.0567	.95	17°	4.10	.0623	2.69
11	2.0	.096	.0565	.76	18°	2.50	.0673	2.67
12	2.0	.096	.0571	.79	17°	2.95	.0747	2.75

0" CLEARANCE - RUDDER RUN REVERSED

8	0.5	.083	.0330	1.06	30°	3.25	.0835	.94
3	1.0	.040	.0455	.97	32°	3.80	.0825	1.66
1	1.0	.096	.0440	.96	27°	3.90	.0640	1.56
2	1.0	.128	.0470	.91	21°	4.20	.0635	1.77
4	1.0	.096	.0490	.90	20°	4.00	.0695	1.92
5	1.0	.096	.0510	.96	20°	4.30	.0735	2.10
7	1.0	.096	.0505	.93	21°	3.90	.0725	2.05
6	1.0	.096	.0500	1.01	27°	3.60	.0595	2.00
10	1.5	.096	.0560	1.03	22°	4.75	.0660	2.62
9	2.0	.096	.0550	.85	17°	4.60	.0542	2.50
11	2.0	.096	.0680	.80	22°	4.00	.0478	5.35
12	2.0	.096	.0650	.82	26°	2.80	.0255	4.00

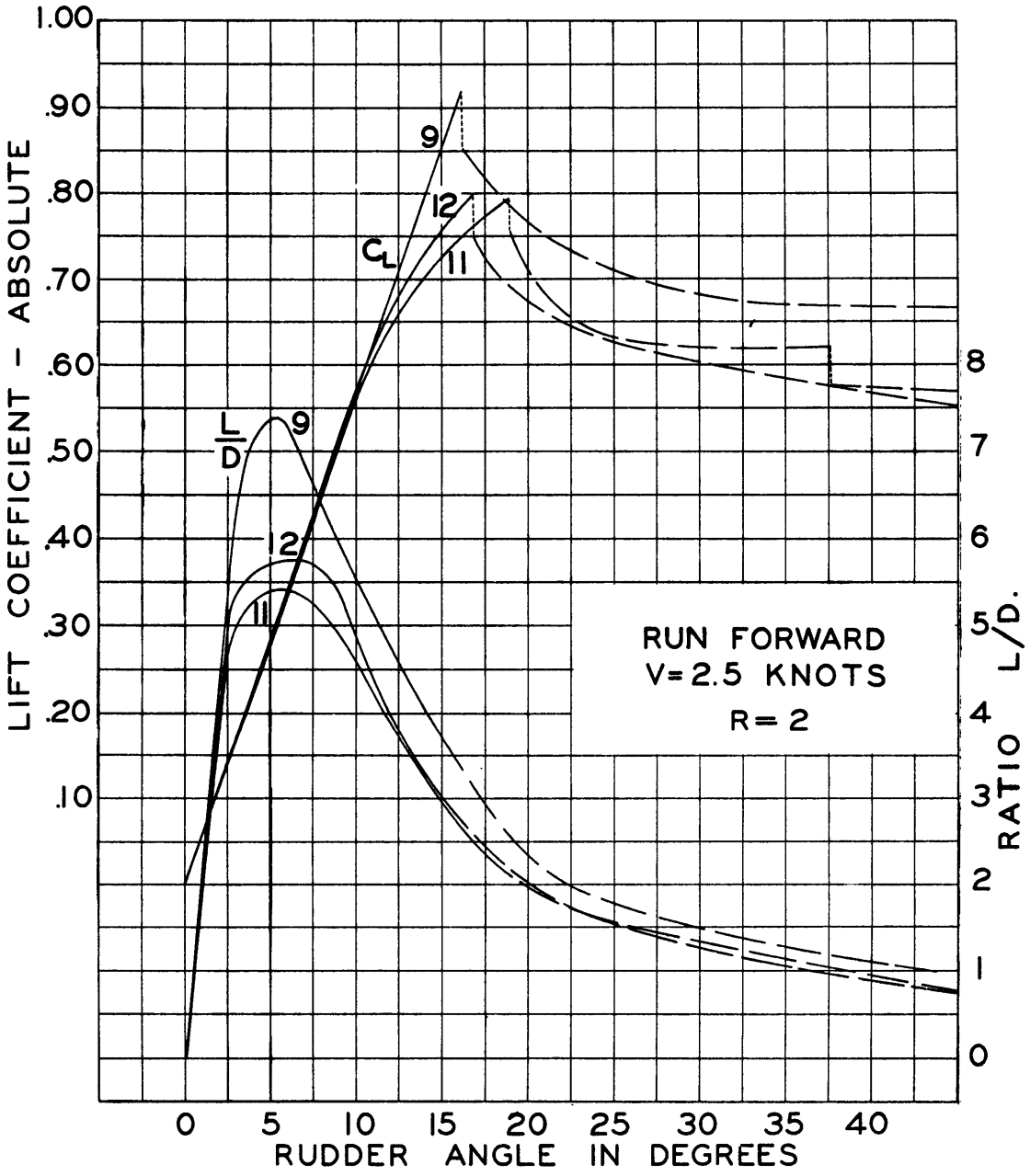

FIG. 25 RUDDERS 9, 11, & 12.

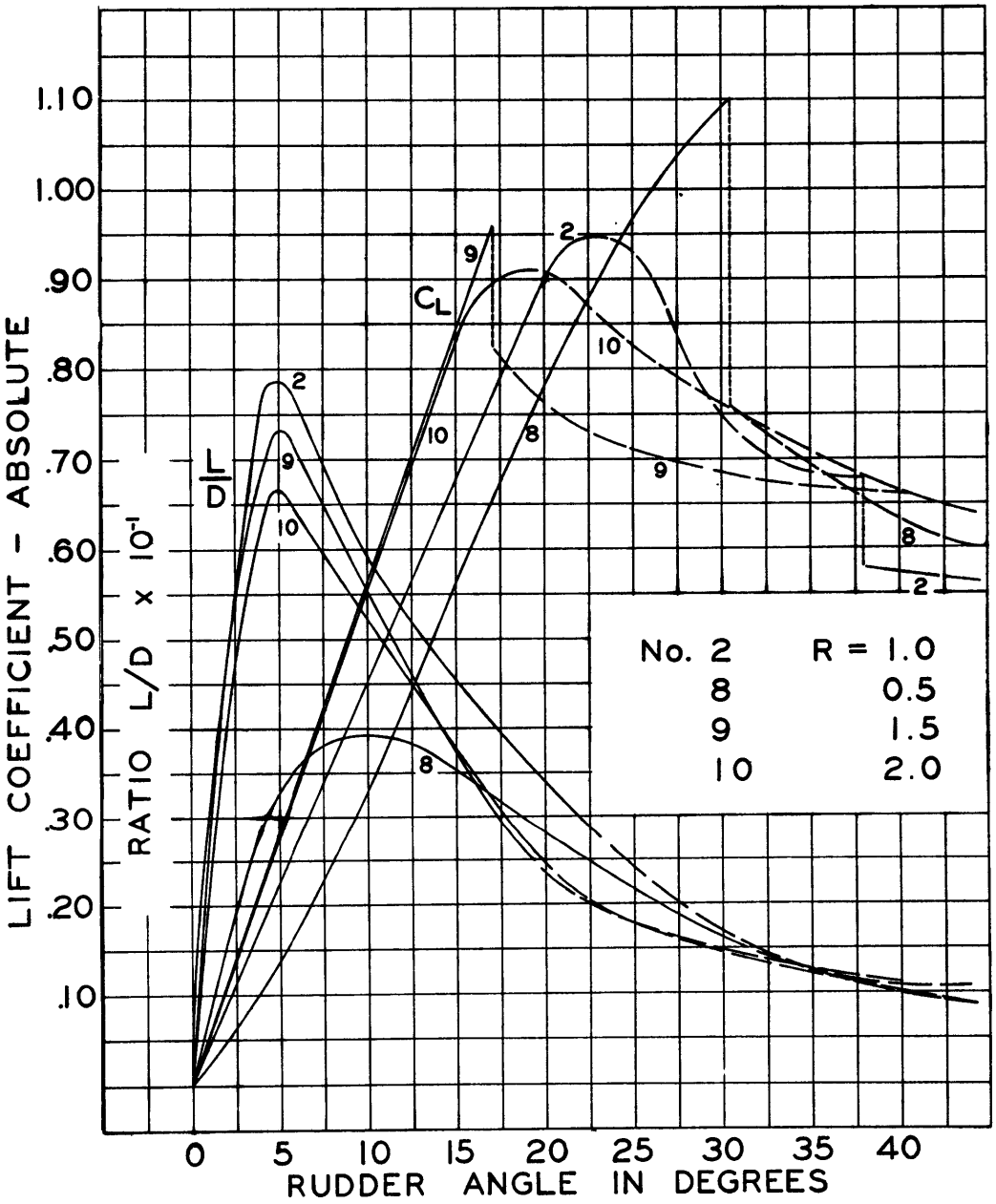

FIG. 26 INFLUENCE OF ASPECT RATIO

FIG. 27.

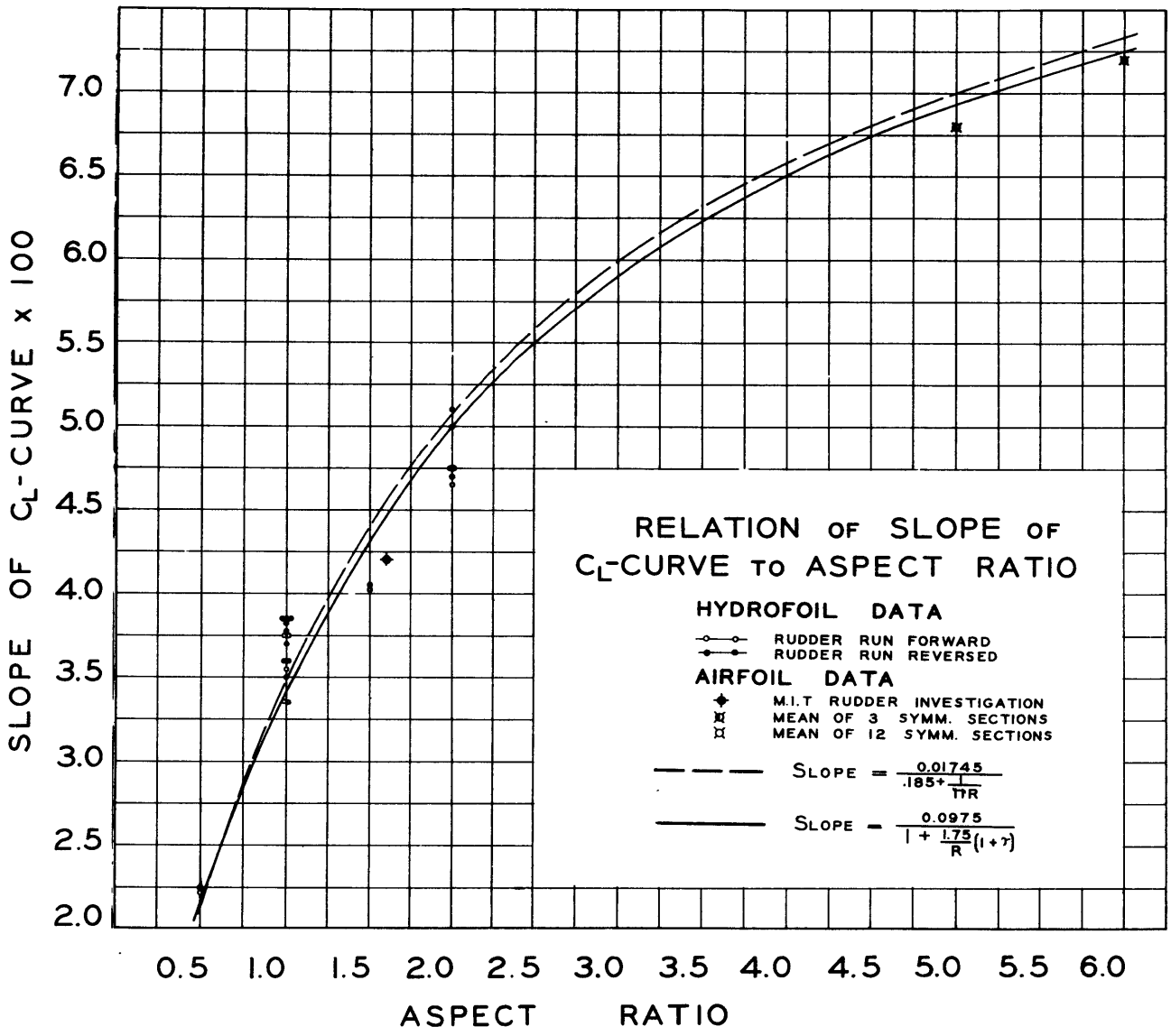
SLOPE OF C_L-CURVE x 100
7.0
6.5
6.0
5.5
5.0
4.5
4.0
3.5
3.0
2.5
2.0
0.5
1.0
1.5
2.0
2.5
3.0
3.5
4.0
4.5
5.0
5.5
6.0
ASPECT RATIO
RELATION OF SLOPE OF C_L-CURVE TO ASPECT RATIO
HYDROFOIL DATA
RUDDER RUN FORWARD
RUDDER RUN REVERSED
AIRFOIL DATA
M.I.T RUDDER INVESTIGATION
MEAN OF 3 SYMM. SECTIONS
MEAN OF 12 SYMM. SECTIONS
SLOPE = $\frac{0.01745}{.185+\frac{1}{\pi R}}$
SLOPE = $\frac{0.0975}{1+\frac{1.75}{R}(1+\tau)}$

The relation between the aspect ratio and the "burble point," that is, the critical angle at which the lift ceases to increase and at which eddies begin to separate from the back of the hydrofoil aft of the leading edge, is shown in Fig. 28.

Lift

The C_L– curve, except in four cases at two inch hull clearance, is practically a straight line until it approaches the neighborhood of the burble point where it flattens out before breaking off abruptly, as it does in most cases, to give lower values. $C_{L_{max}}$, as shown in the tables, varies from 0.64 to 1.23 and, in general, is larger for the smaller aspect ratios. For two inch hull clearance the values of $C_{L_{max}}$ average higher for the rudder run reversed than for forward; for zero clearance the average is about the same in both cases.

The differences in lift coefficient for rudders of various span forms and thickness ratios, but with the same aspect ratio, are negligible as may be seen in Figs. 24 and 25. For R = 1 it will be noticed that the curve for rudder No. 5 (leading edge tapered by 30°) has the greatest slope. In accord with wind tunnel data, the slopes are found to decrease with increasing thickness ratio (rudders 1, 2, and 3) though, to be sure, the difference is small in the range of thickness ratios tested. Tapering of both the leading and trailing edge apparently has the effect of increasing the slope, though this is not true in all cases. These generalizations apply only for the rudder run forward; when the rudder is reversed the thickest rudder is found to have the greatest slope of the three thickness ratios tested.

It is of particular interest and importance to compare the C_L values here obtained with wind tunnel results. Since the slope of the lift coefficient curve will vary with aspect ratio and since practically all airfoil data are given for aspect ratios of five to six, the correlation must take account of this variation. A formula[3] obtained from theoretical considerations which is used for the reduction of wind tunnel results will be used for this purpose, namely:

$$a = \frac{a_o}{1 + \frac{1.75}{R}(1 + \tau)} \qquad (11)$$

where

a = slope of C_L–curve for aspect ratio R

a_o = slope of C_L–curve for infinite aspect ratio and for the section thickness ratio. For a thickness ratio of 0.10 the value used is 0.0975 per degree. This was obtained from aerodynamic data[3].

τ = a factor correcting for the induced angle of

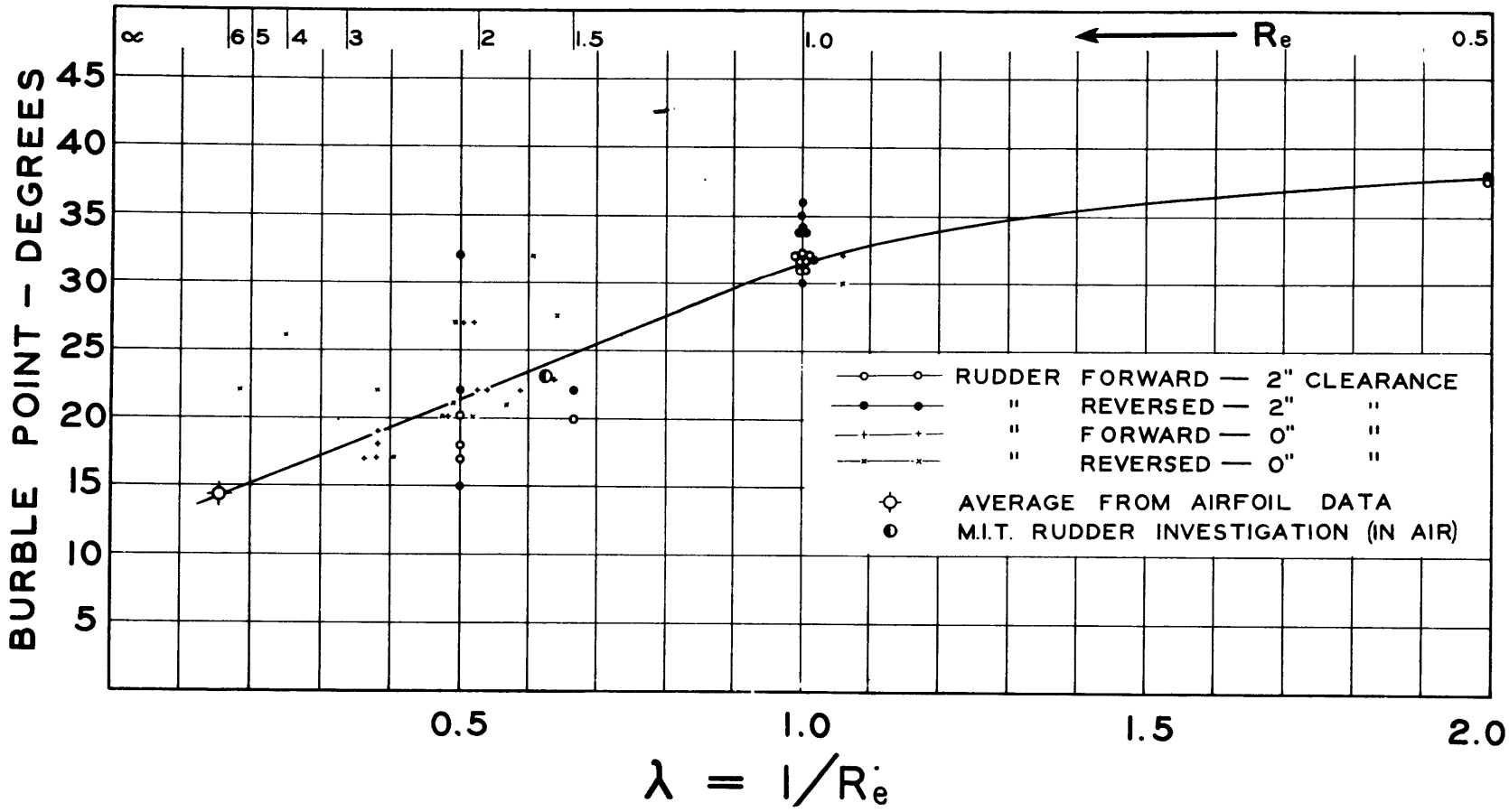

FIG. 28 RELATION OF BURBLE POINT & ASPECT RATIO

attack to allow for departure from elliptical span loading which results from the use of a hydrofoil of rectangular span form.

The factor τ has the following values:

R	τ
0.5	0.03
1.0	.05
1.5	.06
2.0	.08
3.0	.11
4.0	.13
5.0	.16
6.0	.18

Eq. (11) is plotted in Fig. 27 as is also the simplified equation

$$a = \frac{0.01745}{0.185 + \frac{1}{\pi R}} \qquad (12)$$

With these curves the slopes obtained in the test are plotted as are also some averages for symmetrical airfoils[2,4] of aspect ratios 1.6, 5, and 6. The data and the curves representing the equations are in fairly good agreement.

From the curve of Eq. (11) plotted in Fig. 27 the effective aspect ratio R_e corresponding to the values of "a" obtained in the tests with zero hull clearance can be obtained. These are tabulated in Table II. The values found are, in most cases, somewhat less than twice the geometric aspect ratio which is prescribed by theoretical considerations.

In the region immediately past the burble point the C_L-curve has no rational continuity, the value of the lift measured depending upon the Reynolds' number, the degree of turbulence, and other conditions of the test. In a number of cases two or more values were obtained for the same angle of attack that differed by as much as 0.20. Often in the earlier part of a run a given lift would be indicated by the dial gages and as the run continued the readings of the dial gages would slowly decrease till near the terminus of the run a steady value would be reached which was much lower than that at first registered. The former value corresponded approximately to that appropriate to the straight line lift curve of small angles of attack extended.

Drag

The curves of drag coefficient show little but that at angles up to 10° the profile drag C_{D_o} is small and approximately equal to $C_{D_{min}}$ as given by the

equation:

$$C_{D_o} = C_D - \frac{C_L^2}{\pi R_e} \qquad (13)$$

where C_{D_o} = profile drag coefficient and the term $C_L^2/\pi R_e$ gives the magnitude of the induced drag. Above 10° the profile drag increases rapidly and past the burble point, in general, is larger than the induced drag. As a measure of the profile drag and the efficiency of the section the L/D ratios may be compared. As a measure of the efficiency at larger angles, the values of L/D corresponding to $C_L = 0.75$ are given in Tables I and II. The values vary considerably even for rudders of one aspect ratio. Rudders of aspect ratio 1.0 are in most cases more efficient than rudders of higher or lower aspect ratio.

The values of $C_{D_{min}}$, corresponding to $\alpha = 0$, here obtained are all of approximately the same value with the exception of the case of the thick section (rudder No. 2) in which it is greater, and of the flat plate (rudder No. 3) for which it is less. The accuracy of C_D values for angles of less than 10° is not very great because of the smallness of the quantity measured.

Center of Pressure Travel

The center of pressure for all sections and all span forms lies in the region of the quarter chord point at small angles of attack, as is shown in Figs. 12-23. In the case of span forms with the leading edge tapered the position of the center of pressure is measured from the leading edge of the mid-span section.

At zero angle of attack the center of pressure becomes merely the center of resistance, this resistance being made up of two components, namely, frictional resistance and dynamic resistance due to the absence of perfect stream line flow. The center of frictional resistance for these small areas will lie approximately at the center of gravity of the area while the center of dynamic resistance will lie somewhere forward of the position of maximum camber. For symmetrical sections run leading edge forward, the center of resistance, that is, the weighted mean of the two positions, is found to be at approximately the quarter chord point. This is in agreement with wind tunnel tests.

In the case of the rudder run reversed the present tests showed a tendency for the center of pressure to move aft from the quarter chord position as the angle of attack was decreased from about 10°. The total amount of this travel is small, amounting to perhaps five per cent of the chord. Airfoil tests[4] show a travel of as much as 15 per cent of the chord at zero angle of attack, however, center of pressure measurements at small angles are subject to large errors due to the smallness of the forces measured and unless some method of extrapolation similar to that described on page 16 is used, the result obtained is open to question.

With increasing angles of attack, as the burble point is approached the lift coefficient curve will, in general, begin to flatten out and at the same time the center of pressure will move toward the rear. When the burble point is reached the center of pressure will have moved to a point about 40 per cent of the chord length from the leading edge at which position it will remain, approximately, for angles up to 45°. For spans of tapered leading or trailing edges the position of the center of pressure, measured as it is from the forward tip of the mid-span section, will vary a little in position from that it would have for a rectangular span. This variation which is shown in the curves can be easily calculated.

It has been shown by Glauert[17] that satisfactory agreement with experimental results can be obtained if the foil is assumed to be divided into a large number of strips by lines drawn parallel to the chord and if the center of pressure on each strip is assumed to lie at the same fraction of the distance from the leading to the trailing edge of that particular span element. Pressure distribution curves taken over various portions of the span of course show that this assumption does not correspond to the facts in general, but satisfactory final results nevertheless appear to be obtained by its use. The mean position of the center of pressure can be found by simple integration of the elements.

By this method the mean center of pressure position was calculated for the various tapered profiles tested. The deviation of the mean position will vary with the aspect ratio, angle of taper, and the assumed center of pressure for an individual element. It will also be different according to whether the leading or trailing edge is tapered. However, the deviation will be the same for a rudder with the leading edge tapered by a given amount, which is run forward, as for a rudder with the same taper on the trailing edge, run reversed. The calculated deviations are given in the following table.

TABLE III

		Assumed C.P. % chord	Mean C.P. % chord	Deviation % chord
Leading edge tapered 15°	R = 1	25	24.6	-0.6
" " " 15		40	39.7	-0.3
" " " 30		25	23.5	-1.5
" " " 30		40	38.7	-1.3
Trailing edge tapered 15°	R = 1	25	25.1	0.1
" " " 15		40	40.2	0.2
" " " 30		25	25.5	0.5
" " " 30		40	40.8	0.8
Leading edge tapered 15°	R = 2	25	23.2	-1.8
" " " 15		40	38.7	-1.3
" " " 30		25	18.8	-6.2
" " " 30		40	35.0	-5.0
Trailing edge tapered 15°	R = 2	25	25.5	0.5
" " " 15		40	40.9	0.9
" " " 30		25	27.1	2.1
" " " 30		40	43.3	3.3

It is only in the case of the rudders of aspect ratio two that the deviation becomes appreciable. Where it is the leading edge that is tapered, the position of the center of pressure lies nearer the leading edge than it would for a rectangular span; on the other hand, in the case of the trailing edge tapered, the center of pressure lies nearer the trailing edge.

The principal differences in the center of pressure curves can be explained by aid of the table except for the case of tapered rudders of aspect ratio one for which the observed deviation is approximately twice as large as required by the values in Table III. Of course the angle at which the center of pressure travel begins will depend upon the position of the burble point, but for a rudder of rectangular form the center of pressure may be taken as 25 per cent of the chord length from the leading edge at small angles of attack and as 40 per cent of the chord from the leading edge at large angles. For any departures from rectangular span form the shift in the position of the center of pressure can be calculated with sufficient accuracy by Glauert's method.

In the case of a tapered rudder operating in the wake of a ship a further shift in the position of the center of pressure will be engendered by the non-uniform distribution of water velocity over the span. If the wake is known, the position of the center of pressure can be calculated by the insertion of a wake-squared factor in the expression for the area of the span element used in the calculation by Glauert's method.

It will be noticed from the curves for the flat plate (rudder No. 3) that for it the center of pressure at large angles is located further from the leading edge than for the stream line sections. Attention may also be called to the fact that for the condition of the rudder against the hull the center of pressure begins to travel earlier by about 2° or 3° than when clear of the hull.

Moment

The coefficient of moment about the quarter chord point is plotted in Figs. 12-23. Not a great deal need be said about the moment since it is determined by the resultant of lift and drag and by the position of the center of pressure. Since stream line rudders that do not differ widely in aspect ratio, thickness ratio or span form, as for example the range of rudders tested, may be regarded as having approximately the same L/D ratio at the greater angles of attack, the moment corresponding to a given value of lift will depend almost entirely upon the position of the center of pressure, and the axis about which the moment is taken.

In comparison of moments of two or more rudders, the criterion is not the value of the moment coefficient at a given angle of attack but the ratio of the moment (or moment coefficient multiplied by the chord) divided by the lift or lift coefficient. The reason for this is obvious since it is a measure of the

actual torque per unit lift that is essential in rudder design, and rudders of different aspect ratios will have different lifts for a given angle of attack. In Tables I and II this ratio is given for $\alpha = 30°$.

Scale Effect

The data obtained from these tests correspond to a Reynolds' number (vc/ν) of approximately 175,000 if the chord of the rudder is taken as the determining length. However, since the rudder operates partially in the wake of the float, that is, in water which already has a turbulence corresponding to the Reynolds' number of the float, it is somewhat questionable by what value of Reynolds' number the turbulence of the flow about the rudder should be represented. In any case, the fact remains that the Reynolds' number for a full size rudder on a ship would be perhaps 200 times as large as that obtaining in the present tests.

This leads immediately to the question as to how well the curves given here represent the actual forces on a ship's rudder. Aside from the effect of the wake and propeller stream, which would have to be determined for each ship or ship type, a few conclusions as to the effect of scale may be drawn in light of full-scale wind tunnel tests and other data available.

It is fairly safe to say that up to the burble point the effect of scale on the hydrodynamic characteristics is negligible aside from a small decrease in the profile drag at small angles of attack. The position of the burble point has been shown[3] to vary with the velocity and hence will depend upon the scale as well. In general, an increase in velocity will shift the position of burble to higher angles of attack. With this shift only slightly larger values of $C_{L_{max}}$ will appear since the effect is to flatten out the C_L-curve in this extended region[16].

The sharp breaks found at the burble point in model tests, in most cases, resolve themselves into smooth curves giving decreasing values of C_L. In the thick sections a flatter maximum of the C_L-curve is evidenced than in the case of thinner sections, and is reached at slightly greater angles of attack[23]. This tendency is also evidenced in the present tests.

With the retardation of burble at higher Reynolds' numbers there is also a shift in the angle of attack at which the travel of the center of pressure begins. Both of these changes will be dependent upon the scale and velocity and can best be left to direct measurement of full size rudders.

VI CONCLUSIONS

1. The lift coefficient curve may be represented for angles of attack up to the burble point by the equation:

$$\text{Slope} = \frac{0.01745}{0.185 + \frac{1}{\pi R}}$$

The curves for C_L and C_D may be taken to represent equally well the forces on both model and full scale rudder, except that a small decrease in C_D may be expected in the latter case.

2. The variation of the thickness ratio or streamline section makes little difference in the lift and drag below the burble point as long as the thickness ratio does not vary greatly from 10 per cent. Thicker sections give greater drag and smaller lift whereas thinner sections give less drag and greater lift. This is in accord with wind tunnel results.

3. The center of pressure for rectangular span forms can be considered as located at the quarter chord point for small angles and at approximately the 40 per cent chord point for angles past the burble point. Departures from rectangular span form affect only the center of pressure position which can be calculated by the method of Glauert.

4. The torque for a stream line rudder corresponding to a given lift depends almost entirely on the position of the center of pressure and the axis about which the moment is taken.

5. Information other than this, that is, the effect of Reynolds' number, wake of the ship, propeller stream, etc., can only be determined by direct study and measurement of the forces on a full-scale rudder under actual steering conditions.

APPENDIX I

BIBLIOGRAPHY

Symmetrical Sections and Flat Plates

1. Tests of Six Symmetrical Airfoils in the Variable Density Wind Tunnel, E.N. Jacobs, N.A.C.A. Tech. Notes No. 385, 1931.
2. Aerodynamic Characteristics of Airfoils – Symmetrical Sections, Ref. No. 65 N.A.C.A. Tech. Report No. 93, 1920; Ref. Nos. 294, 295, 324, and 325, ibid 124 (1921); Ref. Nos. 506, 507, 508, 558, 559, and 606, ibid 244 (1926); Ref. Nos. 637, 717, 718, 719, and 720, ibid 286 (1928); Ref. Nos. 766, 795, 796, 797, 811, and 812, ibid 315 (1929).
3. Large–Scale Aerodynamic Characteristics of Airfoils, E.N. Jacobs and R.F. Anderson, N.A.C.A. Tech. Report No. 352, 1930. Symmetrical Sections pp. 427 and 428.
4. Investigation of Rudder Action by Wind Tunnel Experiments, H.T. Pfingstag and W.C. Sprenger, Thesis Mass. Inst. Technology 1932.
5. Lift on Flat Plates between Parallel Walls, L. Rosenhead, Roy.Soc., Proc. 132, pp. 127–152, 1931.
6. Flow Past Flat Plates Between Parallel Walls – Applications, T. Sasaki, Phys. Math. Soc. Japan, Proc., 9, pp 68–78, 1927.
7. Resistance of Air, G. Eiffel, Soc. Ing. Civ. France, Bull. 61, pp 261–268, 1908.
8. Flow of Air Behind Inclined Flat Plate of Infinite Span, Roy. Soc., Proc. 116, p 170, 1927. Also B.A.C.A. Annual Report 1927–1928, p 81.
9. Connection Between Lift and Circulation for an Inclined Flat Plate, B.A.C.A. Annual Reports 1927–1928, p 107.
10. General Theory of Thin Wing Sections, Max Munk, N.A.C.A. Annual Report 1922, p 245.
11. Untersuchen mit kreisrunden Platten und ebenen Tragflächen, Zeits. f. Flugtechnik u. Motorluft, 6, p 127, 1915.
12. Two Dimensional Flow past Symmetrical Sections, Brit. Aero. Res. Comm. Report and Memo. No. 1223; Annual Report 1928–1929, p 314.
13. Resistance of Small Plates in a Stream of Fluid, Rayleigh, Phil. Mag. 30, pp 179–181, 1915.
14. Dynamic Pressure on Submerged Flat Plates, H.E. Stevens, Am.Soc.Mech. Eng., J. 39, pp 318–320, 1917.
15. International Critical Tables, Section on Aerodynamics by L.J. Briggs and H.L. Dryden.
16. Tests of Large Airfoils in the Propeller Research Tunnel including Two with Corrugated Surfaces, D.H. Wood, N.A.C.A. Tech. Report No. 336, 1929.

17. B.A.C.A., Report and Memorandum No. 755.
18. Report on Experiments Relative to Rudders, Joessel, Memorial de Genie Maritime, 9, 1873.
19. Le Moment du Resistance du Gouvernail, A Bonnet, Bulletin l'Association Technique Maritime, 1907, pp. 7–15.
20. Full Scale Tests of Rudder Torque, A.J. Maginnis, T.I.N.A. 1886.
21. Thin Blades in Water, R.E. Froude, B.A.C.A. Report and Memo. 1909–1910.
22. Resistance of Thin Plates, T. Stanton, T.I.N.A. 1909.
23. Neuere Gesichtspunkte für den Entwurf von Schiffsrudern, W. Kucharski, S.T.G., 1931, pp.206–257.
24. Variation of Lift and Drag Coefficients with Changes in Size and Speed, W.S. Diehl, N.A.C.A. Annual Reports 7, p. 61, 1921.
25. Scale Effect on Lift, Drag, and Center of Pressure, Brit. Aero. Res. Comm. Reports and Memo. No. 900; Annual Reports 1923–1924, p.507.
26. Dependence of Air and Water Resistance on Velocity, H. Lorenz, Phys. Zeits. 18, pp. 209–214, 1917.
27. Airplane Design, E.P. Warner (1927).

N.A.C.A. National Advisory Committee for Aeronautics
B.A.C.A. British Advisory Committee for Aeronautics
T.I.N.A. Transactions Institute of Naval Architects
S.T.G. Jahrbuch der Schiffbautechnischen Gesellschaft.

APPENDIX II

CALIBRATION of RUDDER DYNAMOMETER

A preliminary calibration of the rudder dynamometer showed a disagreement in the values of the calibration constant obtained for lateral and longitudinal forces (lift and drag), and a further variation of the constant when the distribution of the load on the two springs was changed, as by the application of different torques.

A calibration of the dial gages revealed that their inaccuracies were much too small to produce the discrepancies found. Only one source of error remained, namely, a lack of equality in the stiffness of the two springs. Since the stiffness varies with the fourth power of the diameter, a small difference in the diameter of the two, which might easily occur, would result in a considerable difference in stiffness.

To test the equality of the springs, the balance shown in Fig. 29 was constructed. It consists simply of a frame to which the spring is fastened at one end, and a dial gage to measure the deflection of the opposite end to which is attached a given weight. After comparison, the stiffer spring was thinned down with emery cloth until both springs gave the same deflection under equal loads.

After thus equalizing the two springs the calibration was much more uniform.

Method of Calibration

The calibrating gear used to calibrate the rudder dynamometer is shown in Fig. 30 It is but a support for the dynamometer with provision for applying various lateral and longitudinal forces with varying torques. Different moment arms were available by passing the cord leading to the calibrating weights over the stepped pulley attached to the lower end of the shaft held by the dynamometer.

Calibration showed a linear relation spring deflections as measured by the dial gages, and the applied forces, the proportion between the two being the same for both lift and drag. This constant of proportionality, or calibration constant, was about 5 per cent greater than that found for torque measurements. This can be explained as due to the torsion which takes place in the springs in the case of torque and which does not occur for strictly lateral or longitudinal forces, that is, forces that pass through the center of the stock.

Thus it was necessary to use two calibration constants; F for lift and drag, and F_Q for torque. This is a departure from previous practice in the use of this dynamometer. Formerly some average value of the constant was used for all three.

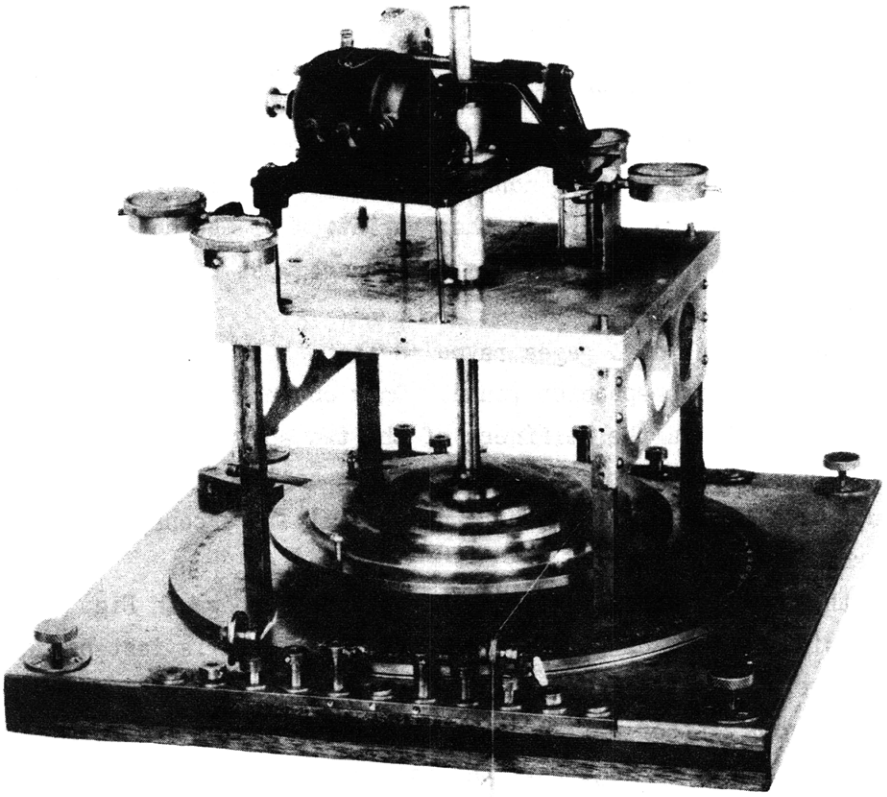

FIG. 30

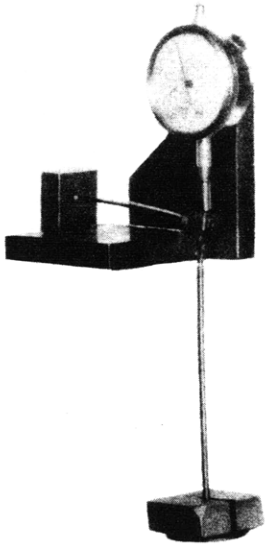

FIG. 29